ORGANOMETALLICS

Article

pubs.acs.org/Organometallics

Synthesis and Structures of Copper(I) Complexes with Phosphino-Functionalized N-Heterocyclic Carbenes (NHCP) and Bis-N-Heterocyclic Carbenes (Bis-NHC)

Erik Kühnel, Igor V. Shishkov, Frank Rominger, Thomas Oeser, and Peter Hofmann*

Organisch-Chemisches Institut, University of Heidelberg, Im Neuenheimer Feld 270, D-69120 Heidelberg, Germany

Supporting Information

ABSTRACT: New copper(I) complexes bearing *N*-phosphino- and *N*-phosphinomethyl-functionalized NHC ligands (NHCP systems) were synthesized and fully characterized. Using halide-containing copper(I) precursors, strikingly different structural motifs were found, dependent on the substitution pattern of the NHCP moiety. An interesting tetranuclear μ_4-bridged copper(I) cluster (**4b**) is formed when $CuBr{\cdot}SMe_2$ is reacted with the *N*-phosphino-substituted ligand **1a**, whereas the dinuclear complex **4a** is formed in an analogous reaction with **1b**. Dinuclear metallacycles (**2a**,**b**) were isolated and characterized by X-ray diffraction when the halide-free copper(I) precursor $[Cu(CH_3CN)_4]PF_6$ was reacted with NHCP ligands **1a**,**b** using the *N*-phosphinomethyl-substituted NHCP ligands **5a**,**b**, as well as employing the bis-NHC ligands BIM and BIM-BMe_2 (**10a**,**b**), respectively. The observed copper(I)−copper(I) distances are directly correlated with the size of the metallacycle formed. An unexpected strong influence upon the metal−metal separation was found for the charged complexes in **10a**,**b**. Using directly *N*-*t*Bu-substituted NHCP ligands led to formation of an electronically less favorable trans-C,C coordination at the copper(I) centers (**3** and **6a**), which inhibited the formation of a dimeric species in the case of **3**.

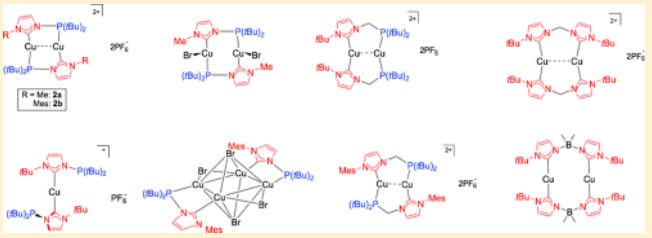

INTRODUCTION

Numerous experimental and theoretical studies have been reported on the structural features of binuclear coinage metal complexes with attractive d^{10}−d^{10} interactions between their metal centers.[1,2] In contrast to Au(I), where correlation effects, strengthened by large relativistic effects, have been proven to play a major role in aurophilicity features,[3] the analogous cupro- and argentophilicities[4] are still a subject of discussion and controversy. Such interactions are sometimes rationalized as "soft" bonding forces arising from hybridization effects between the filled $(n - 1)$d orbitals and the *n*s and *n*p metal orbitals. In some cases, short metal−metal distances in binuclear copper and silver complexes were attributed to steric effects imposed by the ligand, which force two metal centers closer to each other.[5]

Due to their potential in catalysis and also in material science, research on copper(I) complexes bearing bis- or multidentate N-heterocyclic carbene (NHC) ligands has attracted more and more attention in the recent past.[6] A short metal−metal distance has often been found in the solid-state structure of these complexes. In comparison, diphosphinomethane ligands in particular are well-known to support the formation of dinuclear eight-membered-ring systems with intramolecular metal−metal interactions.[7,8] As structural motifs and properties of copper(I) complexes bearing bi- or multidentate ligands are strongly influenced by the steric and electronic properties of the ligands, we have decided to study the chemistry of copper(I) complexes bearing a new hybrid bidentate ligand class, namely P-functionalized NHCs (called NHCP in the following).

The functionalization of NHCs has been a subject of great interest for ligand design and was nicely summarized by Kühl.[9] Interestingly, a theoretical paper by Rösch et al. from 1998 pointed to the possible potential of NHC−phosphine hybrid ligands in Pd-catalyzed Heck reactions.[10] Since the first synthesis of a P-functionalized imidazolium iodide by Herrmann et al.[11] and the actual application of such molecules as precursors for chelating ligands by Nolan et al. in 2003,[12] interest in this field has remarkably increased.[13,14]

Recently, modular synthetic routes were established by our group, which conveniently allowed us to combine phosphines and NHC moieties with a variety of substitution patterns to either *N*-phosphino-[15] or *N*-phosphinomethyl-functionalized[16] NHCP ligands. Two alternative routes disclosed soon after by Kostyuk et al. open alternative ways to remarkably stable *N*-phosphino-substituted NHCPs with widely variable substitution patterns.[17]

We describe the synthesis, solid-state structures, and spectroscopic properties of various unique, two-coordinate, cationic copper(I) complexes, containing NHCP ligands with a direct N−P bond or an *N*-phosphinomethyl substitution

Special Issue: Copper Organometallic Chemistry

Received: July 25, 2012
Published: September 11, 2012

   dx.doi.org/10.1021/om300701u | *Organometallics* 2012, 31, 8000−8011

pattern. The use of such hybrid ligands permitted a detailed look at the steric influence of ligand backbones on the metal−metal interaction of the complex core. Furthermore, we were able to show a significant effect of the overall charges on the copper(I)−copper(I) interaction, using a neutral and an anionic bis-NHC chelate ligand.

RESULTS AND DISCUSSION

Synthesis and Structural Properties of Cationic Copper(I) Complexes with *N*-Phosphino-Substituted NHCP Ligands. When the isolated NHCP systems ^{Me}NHCP^{tBu} and ^{Mes}NHCP^{tBu} (**1a,b**; the superscripts denote the substituents bound to one NHC nitrogen and of the PR_2 at the other NHC nitrogen) were reacted with 1 equiv of $[Cu(CH_3CN)_4]PF_6$ in THF or CH_2Cl_2, complexes **2a,b** (Scheme 1) were obtained in good yields. While the free

Scheme 1

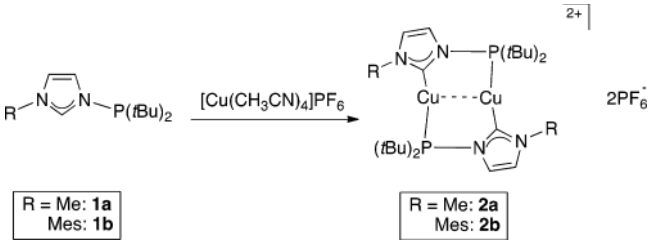

carbenes **1a,b** decompose rapidly when not handled with care under inert and anhydrous conditions, all the NHCP complexes (except **3**) that are reported here are stable in air for weeks. In solution decomposition is observed after several days. Remarkably, complex **2a** is as stable as all of its analogues, although the NHC wingtip is substituted with a small methyl group.

Both molecules are centrosymmetric in the solid state (Figure 1). The NHCP carbene carbon and one phosphine PR_2 donor belonging to different ligand molecules coordinate each copper(I) center. The angles of ca. 174.2° for **2a** and of ca. 177.2° for **2b** found for those fragments hardly deviate from the ideal linear geometry for d^{10}-ML_2 units. The copper(I)−copper(I) distances of 2.613 Å for **2a** and 2.575 Å for **2b**, respectively, are in accordance with a weak intramolecular d^{10}−d^{10} interaction.[3b] An effect of the counterion (PF_6^-) on the copper(I)−copper(I) distance as reported for comparable copper(I) bis-phosphine complexes[7b] can be excluded, since the shortest Cu−F distance found is about 3.67 Å for **2a** and 3.97 Å for **2b**. The steric influence of the substituent on the NHC moiety upon the metal−metal separation is relatively small, since changing the methyl group of **2a** to a mesityl group of **2b** only induces a slight shortening of the metal−metal distance of about 5 pm.

In contrast, enlarging the steric bulk of the NHC moiety by using ^{tBu}NHCP^{tBu} with a voluminous *N*-*t*Bu group (**1c**) results in the mononuclear complex **3**, where one copper(I) center is coordinated in a linear fashion by two separate molecules of **1c** (Scheme 2). The metal center is connected with two different

Scheme 2

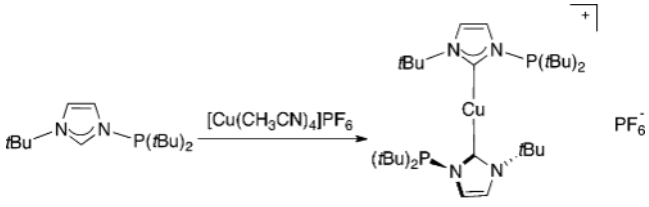

NHCP carbene carbons, while the two corresponding phosphine units remain uncoordinated. Even when the copper(I) precursor was reacted in a 1:1 ratio with ligand **1c**, complex **3** was isolated as the only product.

The twist around the C1−Cu−C21 axis resulting in a dihedral angle between the NHC planes of ca. 75° found in the solid-state structure of **3** minimizes the steric repulsion of two *N*-*t*Bu groups (Figure 2). In order to quantify the steric

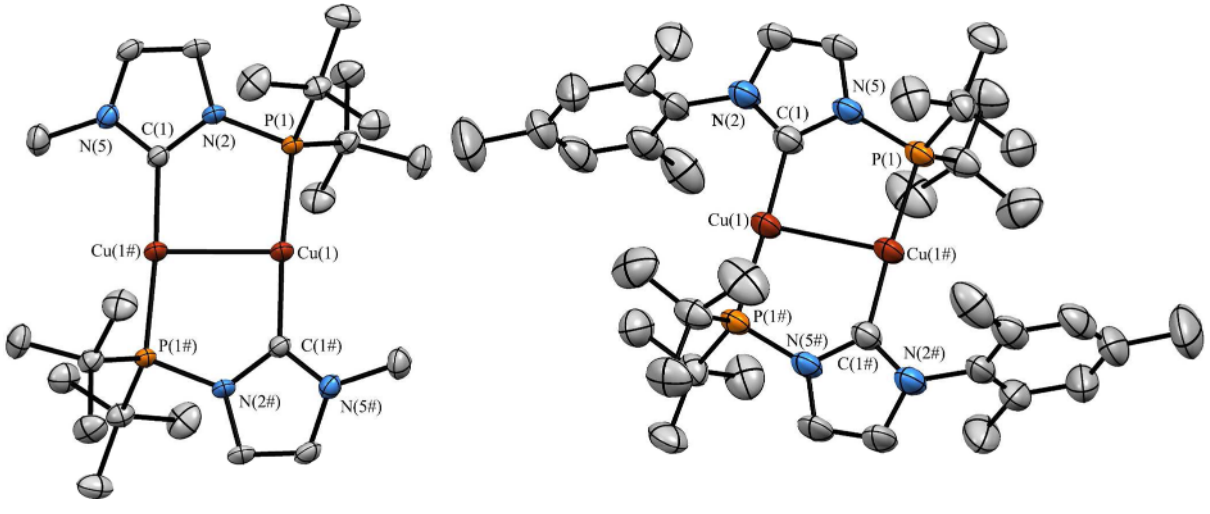

Figure 1. ORTEP plots of **2a** (left) and **2b** (right). Thermal ellipsoids are at the 50% probability level. Hydrogen atoms are omitted for clarity. Selected bond lengths (Å) and angles (deg) of **2a**: Cu(1)···Cu(1#) = 2.6131(5); Cu(1)−C(1#) = 1.9139(19); Cu(1)−P(1) = 2.2022(5); P(1)−N(2) = 1.7379(17); C(1#)−Cu(1)−P(1) = 174.18(6); C(1)−N(2)−P(1) = 121.01(13). Selected bond lengths (Å) and angles (deg) of **2b** (two independent molecules of **2b** were found in the unit cell; the values given are averaged over the two molecules): Cu(1)···Cu(1#) = 2.575; Cu(1)−C(1) = 1.91; Cu(1)−P(1#) = 2.197; P(1)−N(5) = 1.75; C(1)−Cu(1)−P(1#) = 177; C(1)−N(5)−P(1) = 119.

dx.doi.org/10.1021/om300701u | *Organometallics* 2012, 31, 8000−8011

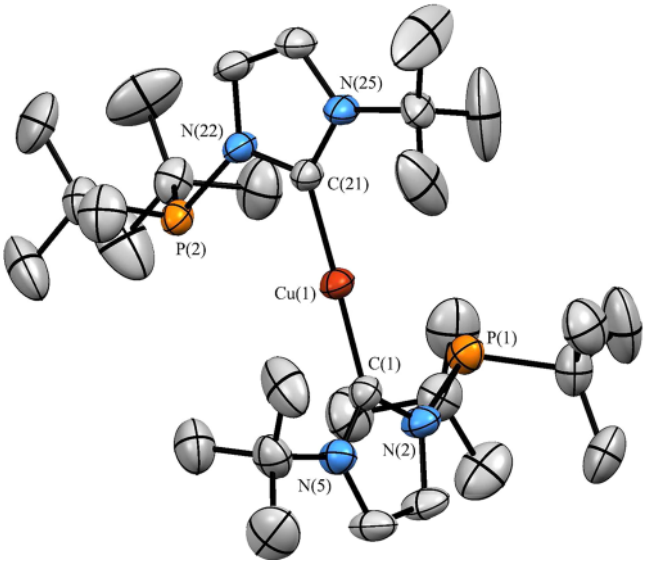

Figure 2. ORTEP plot of **3**. Thermal ellipsoids are at the 50% probability level. Hydrogen atoms are omitted for clarity. Selected bond lengths (Å) and angles (deg) of **3**: Cu(1)−C(21) = 1.904(5); Cu(1)−C(1) = 1.905(4); P(1)−N(2) = 1.756(4); P(2)−N(22) = 1.747(4); C(21)−Cu(1)−C(1) = 178.8(2); C(1)−N(2)−P(1) = 117.3(3); C(21)−N(22)−P(2) = 117.7(3).

demand of different ligands, the so-called "buried volume" (%V_{Bur}) was introduced by Nolan et al.[18] Calculation and comparison of the %V_{Bur} values for different ligand types showed an *N*-*t*Bu-substituted NHC to be bulkier than a P(*t*Bu)$_3$ coordinated to a metal center.[18b] In contrast to NHCs with their NR units pointing toward the metal, phosphines coordinated to metals possess a cone-shaped geometry with P substituents pointing away from the metal center (viz. Scheme 3).[19]

Scheme 3

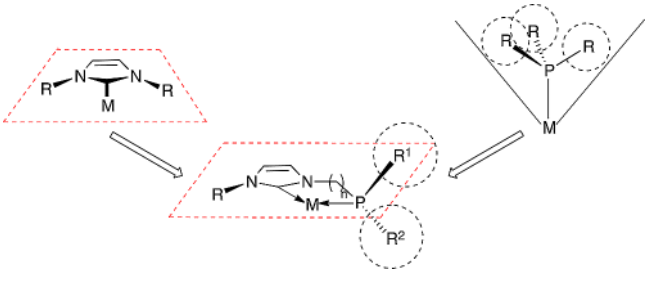

As a result of combining phosphine and NHC ligands in one chelating hybrid system, their individually quite different steric characters generate two different coordination pockets around both ligand atoms coordinating to the metal center. As we have reported previously, the synthesis of an eight-membered dinuclear, dicationic copper(I) metallacycle can be achieved with a diphosphinomethane ligand fully substituted with four *t*Bu groups (dtbpm).[8] In the case of **3** the formation of a dinuclear metallacycle with bridging NHCP ligands is inhibited by the *N*-*t*Bu group on the NHCP, which cannot escape the steric repulsion with the *t*Bu groups of the phosphine arm. The rotational orientation of the two imidazolylidene rings of **3**, which leads to a nearly orthogonal positioning of their planes relative to each other, secures the sterically least repulsive situation. However, as a consequence the coordination of a second copper(I) atom is blocked.

In the ^{1}H NMR spectrum of **3** only one doublet with an integral for 18 protons is detected for all *P*-*t*Bu groups, and the *N*-*t*Bu groups appear as a singlet at 1.71 ppm. No further couplings are detected even at 233 K. The symmetric ^{1}H NMR spectrum in solution certainly arises from the more or less free rotation of the NHCP ligands around the C1−Cu−C21 axis. This dynamic process cannot be frozen out in VT NMR experiments. The phosphorus atoms are detected as a sharp singlet at 101.5 ppm in the ^{31}P NMR spectrum, which is in the range of the free carbene **1c**.[17] The bond angle C(21)−N(22)−P(2) of 117.7(3)° is on the same order of magnitude as those found for **2a**,**b**, which indicates that there is no strain in the ligand backbone of these eight-membered metallacycles.

Synthesis and Structural Properties of Copper(I) Complexes with *N*-Phosphino-Substituted NHCP Ligands and Cu−Br Coordination. When CuBr·S(CH$_3$)$_2$ is reacted with isolated *N*-phosphino-substituted NHCP ligands, the structural motifs of the complexes formed strongly depend on the properties of the involved NHCP ligands. Treatment of **1a** with the thioether-stabilized CuBr reagent in THF afforded copper complex **4a** (Scheme 4).

Scheme 4

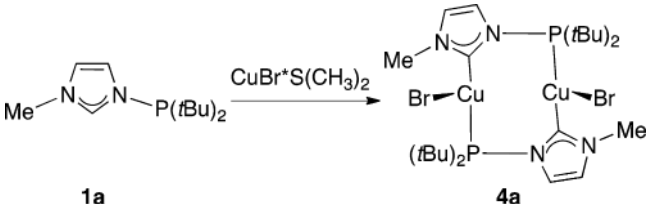

Each copper center is found in a T-shaped ligand environment. A bromo ligand is coordinated to each copper(I) atom in a syn fashion with respect to the metallacycle unit (Figure 3). As a consequence, the metallacycle is folded in a rooflike fashion. Notably, one may draw a parallel between complex **4a** and copper(I)−bis-phosphine complexes described in the literature. In all known cases, the two halide ligands are coordinated in an anti fashion at the copper(I) centers.[7a,c] The only reported copper(I) halide complex with a syn halide arrangement contains a bis-NHC chelate and is an organometallic coordination polymer;[20] dinuclear metallacycles of the type **4a** shown above are—to the best of our knowledge—not known. Similar systems, where NHCs are functionalized either by pyridine[21] or by oxazolinyl[22] side arms, show comparable structures.

The bromo−copper distances are 2.4368(4) and 2.4579(3) Å, respectively, resulting in a significant elongation of the copper−copper distance of **4a** by ca. 0.385 Å (2.9977(3) Å) in comparison to **2a** (2.6131(5) Å). This observation is consistent with the observations described in the literature: the stronger an anion or solvent interacts with copper(I) atoms, the weaker the metal−metal interaction for structurally related compounds.[7c]

Surprisingly, a totally different bonding motif was generated when **1b** was treated with CuBr·S(CH$_3$)$_2$. Even a 1:1 mixture of **1b** and the copper(I) precursor led to the formation of tetranuclear complex **4b** as the only product (Scheme 5). The remaining ligand can easily be washed off the product with

dx.doi.org/10.1021/om300701u | *Organometallics* 2012, 31, 8000−8011

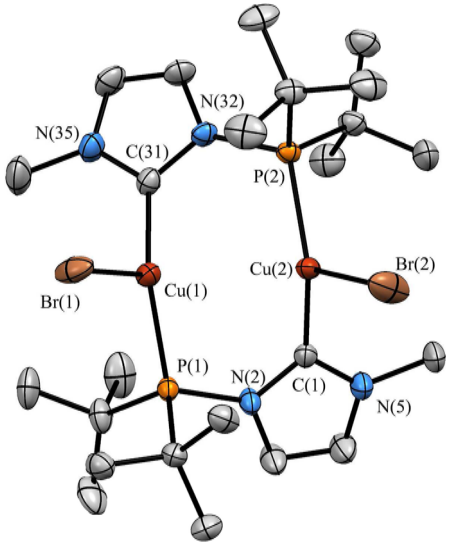

Figure 3. ORTEP plot of **4a**. Thermal ellipsoids are at the 50% probability level. Hydrogen atoms are omitted for clarity. Selected bond lengths (Å) and angles (deg) of **4a**: Cu(1)···Cu(2) = 2.9977(3); Cu(1)−C(31) = 1.951(2); Cu(1)−P(1) = 2.2310(5); P(1)−N(2) = 1.7457(16); P(2)−N(32) = 1.7451(16); C(1)−N(2) = 1.378(3); C(1)−N(5) = 1.352(3); Cu(1)−Br(1) = 2.4368(4); Cu(2)−Br(2) = 2.4579(3); C(31)−Cu(1)−P(1) = 136.43(6); C(31)−Cu(1)−Br(1) = 108.45(6); C(1)−Cu(2)−Br(2) = 109.67(6); P(1)−Cu(1)−Br(1) = 111.50(18); P(2)−Cu(2)−Br(2) = 109.21(2); C(1)−N(2)−P(1) = 120.59(13); C(31)−N(32)−P(2) = 120.12(13).

Et_2O. When **1b** was reacted with $CuBr{\cdot}S(CH_3)_2$ in a 1:2 ratio, **4b** could be isolated in nearly quantitative yield.

Scheme 5

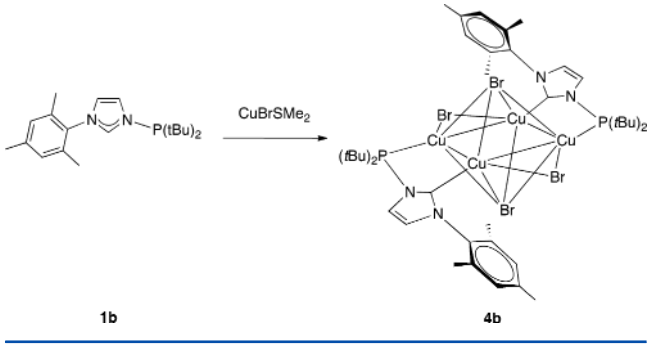

The solid-state structure of **4b** shows a centrosymmetric Cu_4 cluster with a nearly square planar Cu_4 frame (Cu(1), Cu(1#), Cu(2), Cu(2#)), μ_4-bridged on both sides by two bromo ligands, leading to an octahedral substructure (Figure 4). Additionally, two opposite edges of the Cu_4 plane are μ_2-bridged by bromo ligands, whereas the other two edges are bridged by two ligand molecules in a κ^2C,P fashion. The two μ_4-bridging bromo ligands form two short (2.4437(5) and 2.6197(5) Å) and two long (2.7718(5) and 2.8553(5) Å) Cu−Br bonds, so that one μ_4-Br is bending over more to one of the edge-bridging NHCP ligands, while the μ_4-Br on the opposite side of the Cu_4 plane is bending toward the other NHCP bridge (Scheme 5). Each NHCP carbene donor atom is coordinated opposite to the phosphorus center belonging to the other NHCP on the other side. Copper(I) clusters of this kind, where halides are μ_4-bridging a square-planar Cu_4 plane, are quite rare in the literature;[23] those bearing NHC ligands are

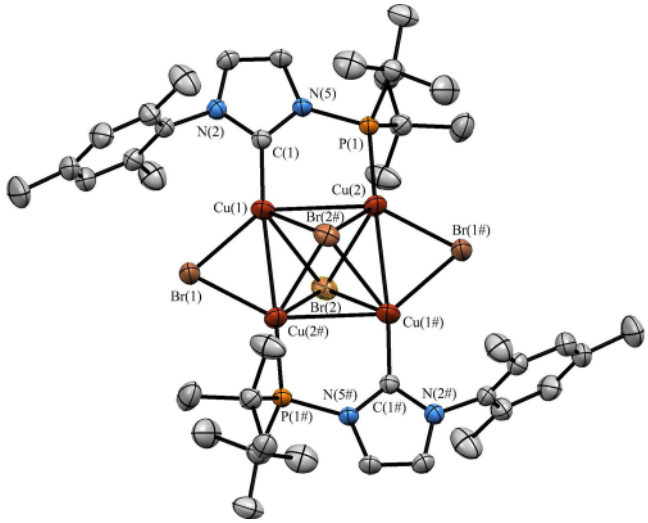

Figure 4. ORTEP plot of **4b**. Thermal ellipsoids are at the 50% probability level. Hydrogen atoms are omitted for clarity. Selected bond lengths (Å) and angles (deg) of **4b**: Cu(1)−Cu(2) = 2.7926(5); Cu(1)−Cu(2#) = 2.7679(5); C(1)−Cu(1) = 1.906(2); P(1)−Cu(2) = 2.1900(7); N(5)−P(1) = 1.744(2); Cu(1)−Br(1) =2.4437(5); Cu(2#)−Br(1) = 2.6197(5); Cu(1)−Br(2) = 2.8553(5); Cu(2)−Br(2) = 2.7718(5); Cu(2#)−Br(2) = 2.4839(4); Cu(1#)−Br(2) = 2.6197(5); C(1)−Cu(1)−Cu(2b) = 168.11(8); P(1)−Cu(2)−Cu(1#) = 167.77(3); C(1)−N(5)−P(1) = 118.97(16).

unknown. The Cu_4 plane spans a parallelogram with two different copper(I)−copper(I) distances. The μ_2-bromo-bridged copper centers are separated by 2.7679(5) Å, whereas the distance between the NHCP-bridged copper centers is 2.7926(5) Å. The four copper(I) atoms, the bridging NHCP ligands, and the μ_2-bridging bromo ligands are in one plane. As expected, the mesityl ring planes are nearly orthogonal to the NHC planes. As visible in the displayed solid-state molecular structure of **4a** (Figure 3), the rooflike structure of this dinuclear halide coordinated metallacycle brings the *N* substituents of the two NHCP units closer together than in the cationic systems such as **2a,b**. Hence, the increase of the steric bulk, from *N*-methyl in **4a** to *N*-mesityl in **4b**, may prevent the formation of just dinuclear complexes in the halide-containing systems.

Synthesis and Structural Properties of Cationic Copper(I) Complexes with *N*-Phosphinomethyl-Functionalized NHCP Ligands. Introducing a methylene bridge between the phosphine donor center and the NHC nitrogen of NHCP ligand systems increases the flexibility of the ligand backbone. For this second type of chelate ligand the superscripts of e.g. $^{tBu}NHC(CH_2)P^{tBu}$ denote the substituents bound to an NHC nitrogen and the P substituents of the CH_2−PR_2 unit at the other NHC nitrogen. The consequences of the structural modification of the NHCP ligands upon the copper(I)−copper(I) separations are discussed below.

When isolated 3-*tert*-butyl-1-(di-*tert*-butylphosphinomethyl)-imidazol-2-ylidene (**5a**; $^{tBu}NHC(CH_2)P^{tBu}$) was reacted with $[Cu(CH_3CN)_4]PF_6$, the dinuclear, cationic copper(I) complex **6a** was formed in good yield (Scheme 6).

In the solid-state structure of **6a**, two different copper(I) centers are present. One is coordinated by two NHC carbon atoms, while the other is coordinated by two P atoms (Figure 5). In the solid state, the dication of **6a** shows crystallographic C_2 symmetry. The copper(I)−copper(I) separation of 2.636(3)

dx.doi.org/10.1021/om300701u | *Organometallics* 2012, 31, 8000−8011

Scheme 6

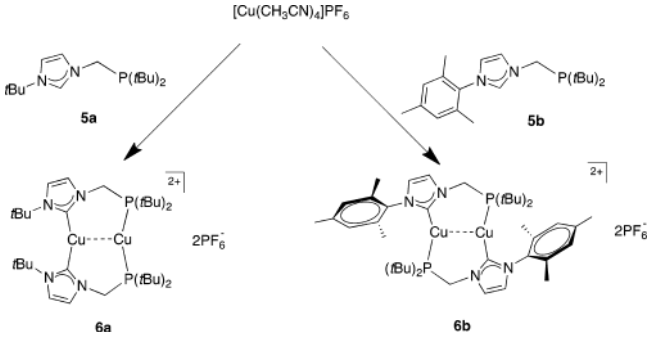

Å is in the same range as for complexes **2a**,**b** and is thus in accordance with a weak interaction of the two d^{10}-metal centers. This interaction is also reflected in a nonlinear P−Cu−P angle of ca. 166° and a C_{NHCP}−Cu−C_{NHCP} angle of ca. 174°. The counterintuitive, normally less expected, electronically disfavored trans position of two stronger σ-donors on the same metal center turns out as being due to the most efficient minimization of steric repulsion between the *N*-*t*Bu substituents in the observed structure. In the alternative structure with trans positioning of P and C_{NHCP} at each copper, the *N*-*t*Bu moieties cannot escape severe repulsion with the *t*Bu groups at phosphorus. As is apparent from Figure 5, the observed structure of **6a** avoids pathologically close *N*-*t*Bu/*N*-*t*Bu contacts by distorting the two imidazolylidene rings around the C_{NHCP}−Cu(1)−C_{NHCP} axis. On coordination trans to a phosphine unit, a similar distortion of the imidazolylidene ring planes would not minimize the steric repulsion due to the conical shape of the phosphine moiety (vide supra). In contrast to the linear compound **3** with two independent *N*-phosphino-substituted ligands ^{tBu}NHCP^{tBu} (**1c**) and a torsion angle of 75°, where dimer formation is presumably prevented by the higher rigidity of the ligand backbone, the introduction of a methylene bridge in the ligand backbone of **5a** allows the relative distortion of the imidazolylidene planes to be 99° within the formed 10-membered metallacycle in **6a**.

This distortion of the imidazolylidene rings leads to the formation of a chairlike conformation, which remains rigid even in solution. The diastereotopic CH_2 protons of the methylene bridges are detected as two doublets at 4.98 and 4.49 ppm in the ^{1}H NMR spectrum of **6a** at 295 K. Two different *P*-*t*Bu groups are detected as pseudotriplets at 1.35 and 1.20 ppm. The *N*-*t*Bu groups appear as one singlet at 1.65 ppm. In the ^{13}C NMR spectrum the two NHC carbene carbons give rise to one singlet at 170.0 ppm, which is in the characteristic range of copper(I) NHC complexes.[6,24]

The corresponding reaction of $[Cu(CH_3CN)_4]PF_6$ with the phosphinomethyl-substituted ^{Mes}NHC(CH$_2$)P^{tBu} (**5b**) gives complex **6b** in good yields (Scheme 6). In contrast with **6a**, each copper center is connected to one phosphine and one carbene donor of different ligand molecules. The mesityl ring planes are orthogonal to the NHC planes, which decreases the spatial demand directed to the copper(I) centers (Figure 5). Here a trans-C,P coordination at each Cu(I) is possible, in accordance with our findings for complexes **2a**,**b** and **3**.

The absence of the *N*-*t*Bu groups functioning as conformational anchors is also reflected in the ^{1}H NMR spectrum of **6b**. At 295 K, the C4/C5 imidazole protons give rise to two singlets with equal intensity at 7.52 and 7.03 ppm. The aromatic mesityl protons appear as one singlet at 6.99 ppm with intensity double that of the imidazolyl protons. The protons of the methylene bridges appear as a singlet at 4.89 ppm. The mesityl CH_3 protons resonate as singlets at 2.30 ppm for the para and 1.94 ppm for the ortho groups with the correct integrals. For all *P*-*t*Bu groups only one doublet at 1.10 ppm is detected, indicating a fluxional system in solution at 295 K.

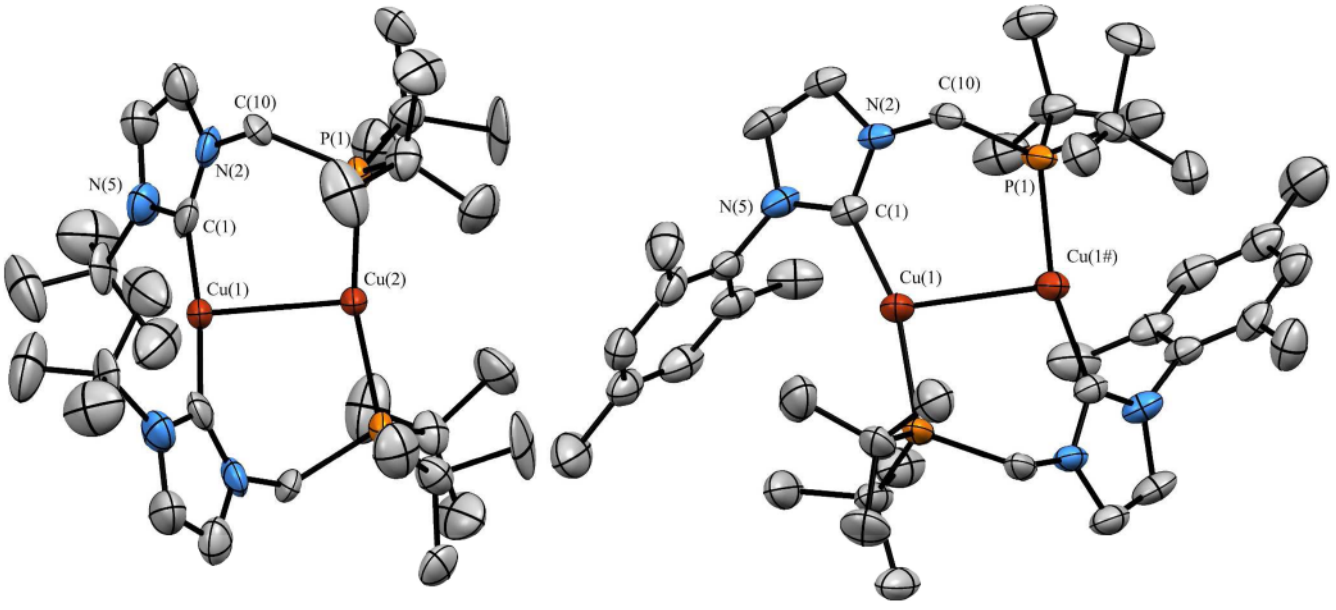

Figure 5. ORTEP plot of the dications **6a** (left) and **6b** (right). Thermal ellipsoids are at the 50% probability level. Hydrogen atoms are omitted for clarity. Selected bond lengths (Å) and angles (deg) of **6a**: Cu(1)···Cu(2) = 2.636(3); Cu(1)−C(1) = 1.929(16); Cu(2)−P(2) = 2.249(4); C(1)−Cu(1)−C(1#) = 173.6(9); P(1)−Cu(2)−P(1#) = 166.1(2). Selected bond lengths (Å) and angles (deg) of **6b** (two independent molecules **6b** were found in the unit cell; the values given here are averaged over the two molecules): Cu(1)···Cu(1#) = 2.744; Cu(1)−C(1) = 1.92; Cu(1)−P(1#) = 2.22; C(1)−Cu(1)−P(1#) = 166.3.

dx.doi.org/10.1021/om300701u | *Organometallics* 2012, 31, 8000−8011

Scheme 7

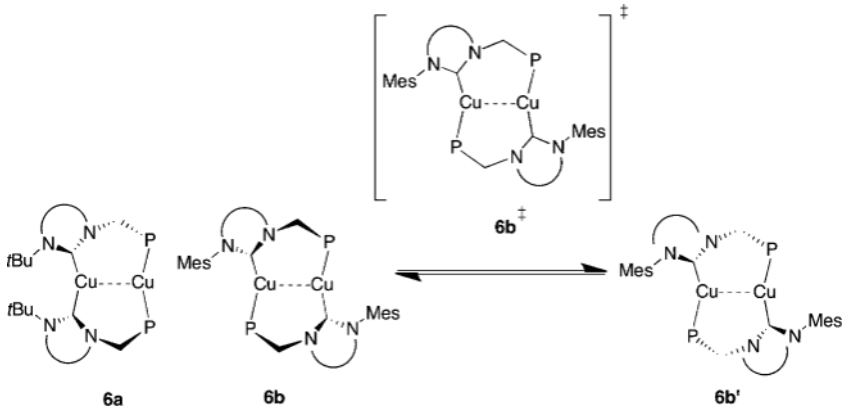

Since no strong solvent influence upon NMR spectra was found for complex **6b** (it exhibits very similar ^{1}H and ^{31}P chemical shifts in CD_3CN and CD_2Cl_2), the observed spectra clearly point to a distinct conformational flexibility of **6b**. The presence of a conformational anchor such as an *N*-*t*Bu group results in a significant decrease of symmetry in the ^{1}H NMR spectrum of **6a**. We assume that the dynamic behavior of **6b** in solution is a stereoisomerization process proceeding via the C_i-symmetrical transition state **6b**‡, responsible for the time-averaged symmetric spectra (Scheme 7).

Looking more closely into the structural dynamics of **6b** in solution, we find that the low-temperature (183 K) ^{1}H NMR spectrum of **6b** is consistent with the solid-state structure determined by X-ray crystallography. Slow cooling of a solution of **6b** in CD_2Cl_2 from 295 to 183 K led to the separation of the signals detected for the methylene protons of the ligand backbone. The two protons now give rise to two singlets at 3.92 and 3.33 ppm, respectively. A further resolution of these signals, as expected for diastereotopic methylene protons, could not be detected. The reduction of symmetry of **6b** at lower temperature is also reflected in the separation of the signals for the *o*-CH_3 mesityl protons, which resonate as two singlets at 1.62 and 1.37 ppm at 183 K. The *P*-*t*Bu groups resonate as two broad singlets at 1.03 and 0.67 ppm at 183 K), which indicates the presence of two different *P*-*t*Bu groups, one in an equatorial and one in an axial position. The activation barrier for this fluxional process as derived from ^{1}H-VT NMR spectroscopy was found to be $\Delta G^{‡} = 46.0 \pm 1.0$ kJ/mol (Figure 6).

We were not able to determine whether a comparable fluxional process at higher temperatures is operative also for **6a** via VT NMR, due to its poor solubility in suitable solvents.

Synthesis and Structural Properties of Cationic Copper(I) BIM and Neutral BIM-BMe$_2$ Complexes. Already in 2001, Fehlhammer et al. reported a neutral dinuclear gold(I) complex bearing a formally anionic bis-NHC borate ligand, where no metal−metal interaction was observed.[25] Using comparable bis-NHC ligands for the synthesis of macrocyclic copper dimers, strikingly different copper−copper distances were found depending upon the total charge of the complexes. We prepared the imidazolium precursors bis(3-butylimidazolium-1-yl)methane dibromide (**8a**; BIM(H_2)) and bis(3-*tert*-butylimidazolium-1-yl)dimethylborate bromide (**8b**; BIM(H_2)-BMe_2) by quaternization of *N*-*tert*-butylimidazole with CH_2Br_2 or $(CH_3)_2BBr$ (Scheme 8).[20]

Treatment of **8a** in methanol with NH_4PF_6 resulted in complete substitution of bromide for the hexafluorophosphate anion and in the formation of the salt **9**. Deprotonation of this salt either using KO*t*Bu or *n*BuLi, followed by a reaction with $[Cu(CH_3CN)_4]PF_6$, yielded the 12-membered, dinuclear, dicationic copper complex **10a**. In the solid-state structure the dication of **10a** only slightly deviates from molecular C_2 symmetry. Each copper atom is connected to two non-equivalent carbene carbons of different ligand molecules (Figure 7). The copper(I)−copper(I) separation of 2.8660(4) Å is on average about 16 pm longer than for the analogous cationic copper(I) complexes with *N*-phosphinomethyl-substituted NHCP and on average about 27 pm longer than for the *N*-phosphino-substituted NHCP. This might be a result of further enlarging the metallacycle. As already found for complexes **3** and **6a**, the imidazolylidene rings are orientated in an almost perpendicular fashion relative to each other. Since two NHC rings are connected via a methylene bridge, a boatlike conformation for the metallacycle is formed. The *N*-*t*Bu groups act as conformational anchors.

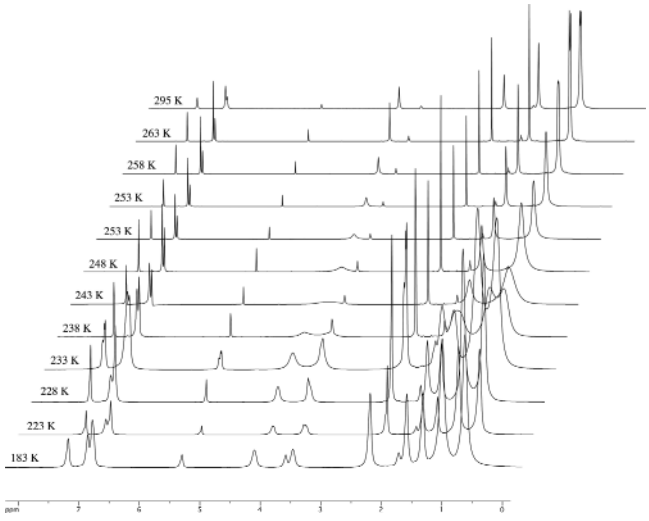

Figure 6. ^{1}H-VT NMR (500 MHz) spectrum of **6b** in CD_2Cl_2. Signals at 3.58 and 1.72 ppm can be assigned to traces of THF.

The low-temperature (213 K for ^{1}H and 234 K for ^{13}C) NMR spectra of compound **10a** are consistent with this observation. In the ^{1}H NMR spectrum, the eight C4/C5 imidazolylidene protons give rise to four slightly broadened singlets with equal intensity at 7.57, 7.46, 7.33, and 7.24 ppm. The methylene protons appear as two sets of doublets at 6.51 and 6.30 ppm with a geminal coupling constant of $^{2}J_{H,H} = 14$

dx.doi.org/10.1021/om300701u | *Organometallics* 2012, 31, 8000−8011

Scheme 8

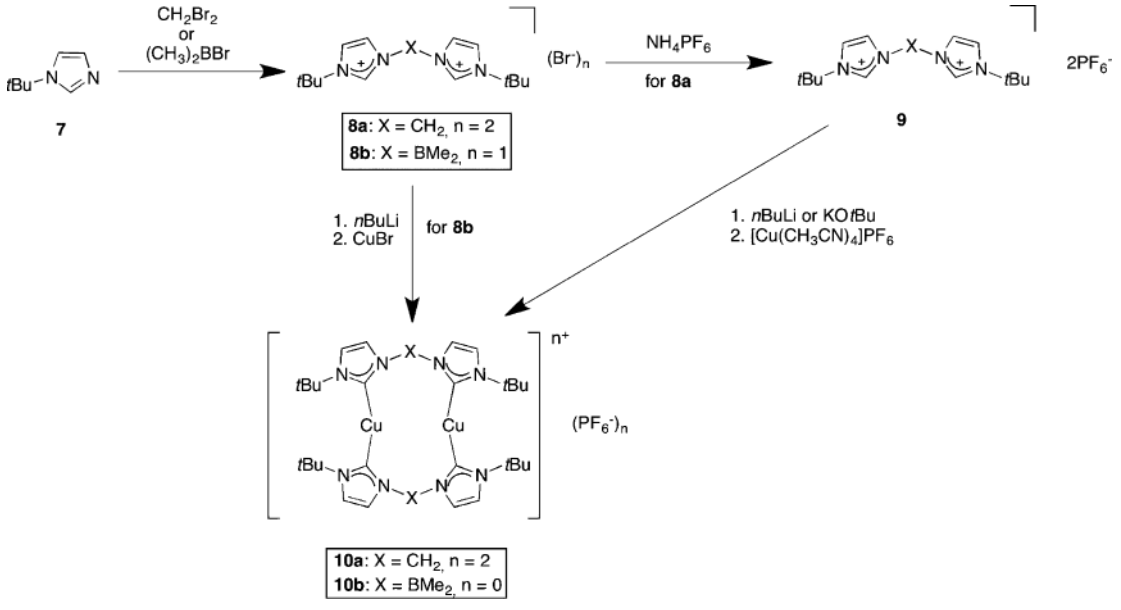

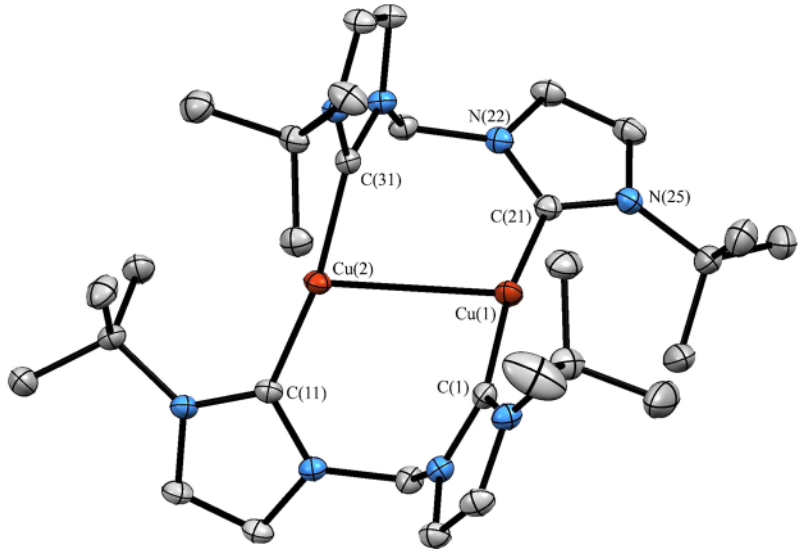

Figure 7. ORTEP plot of the dication of **10a**. Thermal ellipsoids are at the 50% probability level. Hydrogen atoms are omitted for clarity. Selected bond lengths (Å) and angles (deg): Cu(1)···Cu(2) = 2.8660(4); Cu(1)−C(1) = 1.9155(19); Cu(1)−C(21) = 1.9172(19); Cu(2)−C(11) = 1.920(2); Cu(2)−C(31) = 1.921(2); C(1)−Cu(1)−C(21) = 167.00(8); C(11)−Cu(2)−C(31) = 168.89(8).

Hz, and two *t*Bu groups result in two intense singlets at 1.66 and 1.47 ppm, demonstrating a C_2 symmetry of the molecule in solution. The two nonequivalent carbenoid carbons resonate at 173.9 and 172.4 ppm in the ^{13}C NMR spectrum, which is again in the characteristic range of copper(I) NHC complexes. Slow warming of the cooled solution of **4a** in CD_2Cl_2 from 213 to 295 K leads to a coalescence of all signals in the ^{1}H NMR spectra (Figure 8). A fluxional process leading to a symmetry apparently higher than that observed in the solid state is thus fast on the NMR time scale at room temperature.

This fluxional process presumably is the same as that discussed for **6b**. The stereoisomerization of two conformers via a C_{2v}-symmetrical transition state for **10a** is shown in Scheme 9. The 12-membered metallacycle should be more flexible than the 10-membered ring, which might be the reason why coalescence is observed at much lower temperatures in comparison to **6a**, although the NHC units are substituted with *t*Bu groups.

The Gibbs free activation barrier derived from ^{1}H-VT NMR spectra was found to be $\Delta G^{\ddagger} = 53.4 \pm 1.2$ kJ/mol. At 295 K the ^{13}C NMR spectrum of compound **10a** exhibits only one signal for the carbene carbons at 174.2 ppm.

Reaction of the salt **8b** with 2 equiv of *n*BuLi, followed by treatment with 1 equiv of CuBr, afforded the neutral, dinuclear complex **10b** (Scheme 8).

The solid-state structure of **10b** is similar to the structure of the corresponding cationic dimer **10a**. Both complexes have nearly identical Cu−C_{NHCP} and N−C_{NHCP} distances. The large copper(I)−copper(I) separation of 3.418(1) Å found in **10b**, however, excludes any attractive d^{10}−d^{10} metal−metal interaction (Figure 9). The average B−N distance (1.588 Å) is longer by 0.135 Å than the average CH_2−N distance (1.452 Å)

dx.doi.org/10.1021/om300701u | *Organometallics* 2012, 31, 8000−8011

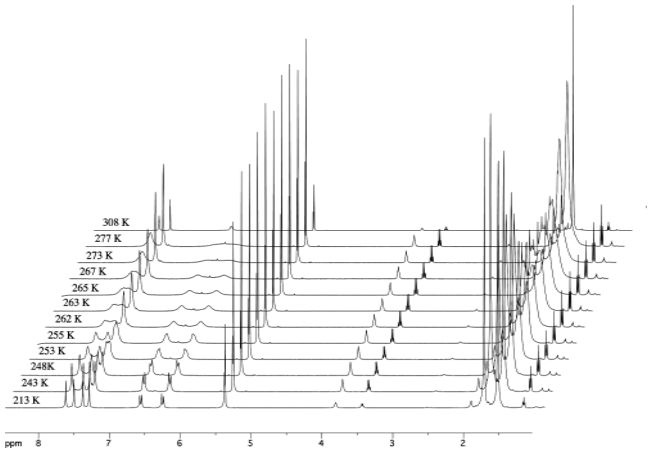

Figure 8. ^{1}H-VT NMR spectrum (500 MHz) of **10a** in CD_2Cl_2. The signals at 3.38 and 1.13 ppm can be assigned to traces of Et_2O.

Scheme 9

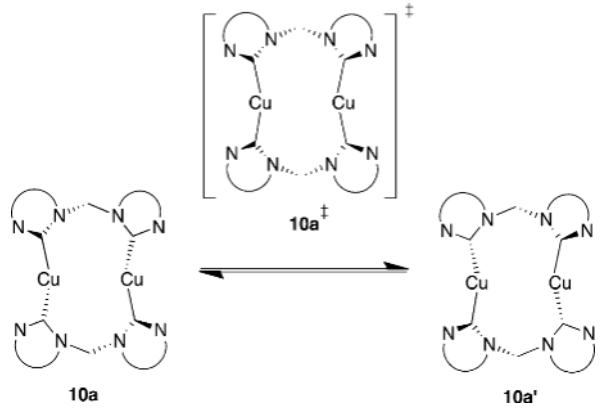

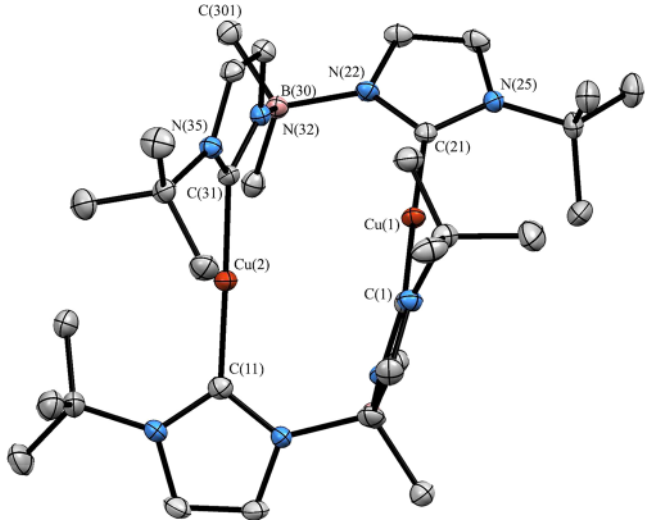

Figure 9. ORTEP plot of **10b**. Thermal ellipsoids are at the 50% probability level. Hydrogen atoms are omitted for clarity. Selected bond lengths (Å) and bond angles (deg) of **10b**: Cu(1)···Cu(2) = 3.4176(6); Cu(1)−C(1) = 1.917(3); Cu(1)−C(21) = 1.919(3); Cu(2)−C(11) = 1.920(3); Cu(2)−C(31) = 1.927(3); B−CH_3 range 1.603(4)−1.620(4); C(1)−Cu(1)−C(21) = 176.12(11); C(11)−Cu(2)−C(31) = 178.48(11).

in complex **10a**, and the N−B−N angles (105.9−106°) are smaller by ca. 6° than the corresponding N−CH_2−N angles (112.1−113.1°). Neither solvent nor LiBr coordination was found in the solid state.

The spectroscopic properties of compound **10b** are very similar to those of **10a**. Low-temperature ^{1}H and ^{13}C NMR spectra correspond to the solid-state structure. Two different CH_3 groups at boron and *t*Bu groups at N give rise to two couples of singlets at 0.13, 0.63 ppm and 1.36, 1.66 ppm in ^{1}H NMR spectra, respectively. Eight imidazole protons resonate at 6.87, 6.99, 7.04, and 7.10 ppm. As in the case of compound **10a**, slow warming of the sample of **10b** led to a coalescence of all related signals in the ^{1}H NMR spectrum. The activation barrier (derived from ^{1}H-VT NMR spectra) for this fluxional process, which has the same reason as discussed for complex **10a**, was found as $\Delta G^{\ddagger}$ = 47.9 ± 0.9 kJ/mol.

SUMMARY

A series of mono- and dinuclear copper(I) complexes, both cationic and neutral, with *N*-phosphino- and *N*-phosphinomethyl-substituted NHCP ligands were synthesized and fully characterized. The structural properties of the new complexes strongly depend on the steric bulk of the NHC moiety of these ligands. In the case of the reaction of $[Cu(CH_3CN)_4]PF_6$ with the carbenes **1a**,**b**, symmetric, dinuclear eight-membered metallacycles (**2a**,**b**) were obtained, whereas the formation of a dinuclear species was inhibited in the case of the *N*-*t*Bu substituted NHCP **1c** due to steric repulsion (**3**). Short copper(I)−copper(I) distances of 2.61 and 2.57 Å were found for complexes **2a**,**b**, presumably as a result of the rigidity and small bite angles of the ligands leading to close preorganization of the copper(I) centers. The effect of varying the N substitution of *N*-phosphino NHCP ligands on the metal−metal separations, as well as on the stability of the compounds, was marginal. Enlarging the ring size of the dinuclear metallacycles by using *N*-phosphinomethyl-functionalized NHC ligands (**6a**,**b**) resulted in an increase of the metal−metal separation of ca. 0.16 Å for the 10-membered dicopper metallacycles. Further enlargement of the metallacycles by the use of the bis-NHC ligands BIM and BIM-BMe_2 in complexes **10a**,**b** expanded this distance by an additional 0.11 Å. Hence, a short copper(I)−copper(I) distance in these dinuclear dicopper(I) metallacycles is related to the flexibility of the NHCP ligand backbone, while the coordination geometry (trans-C,C vs trans-C,P NHCP coordination at Cu(I)) is solely determined by the substitution pattern of the ligand and by sterics.

The strong effect of the NHCP substitution pattern upon the observed structural motifs is also reflected when halide-containing copper(I) sources were reacted with the free carbenes **1a**,**b**. The neutral dinuclear complex **4a** was obtained when the *N*-methyl-substituted NHCP ligand **1a** was reacted with $CuBr{\cdot}S(CH_3)_2$. This metallacycle, in which the bromo ligands coordinate to two different copper(I) atoms, is comparable to well-known dinuclear bis-phosphine halide copper(I) complexes described in the literature.[7,8] Surprisingly, when the NHCP ligand **1b** is reacted with the same copper(I) source, an unusual Cu_4 cluster was isolated in nearly quantitative yield. Only three examples of such clusters, where a planar Cu_4 unit is halide bridged in a μ_4 fashion, have been reported in the literature.[21]

A significant influence of the overall complex charge on copper(I)−copper(I) interactions was revealed by the use of bis-NHC ligand systems BIM and BIM-BMe_2 for the synthesis of isoelectronic cationic and neutral dinuclear copper(I)

dx.doi.org/10.1021/om300701u | *Organometallics* 2012, 31, 8000−8011

metallacycles, respectively. The elongation of the metal−metal distance from 2.87 Å in **10a** to 3.42 Å in **10b** can hardly be explained by mere steric effects imposed by the ligand backbone of BIM-BMe$_2$ in comparison to BIM, since there are only marginal differences between the steric characteristics of the two ligands. An effect of solvent−anion interaction at the metal centers as a reason for the strikingly different metal−metal separations found for **10a,b** could also be excluded from the solid-state molecular X-ray structure determinations.

In summary, the copper(I)−copper(I) distances of the systems investigated here in the solid state significantly depend upon the ring size, the steric properties, the substitution patterns of the NHCP ligands, and the overall charges of the metallacycles. The use of the hybrid NHCP makes the isolation and full characterization of a variety of stable, novel copper(I) complexes possible. The reactivity of these systems in e.g. homogeneous catalysis is being investigated in our laboratories.[26] A theoretical treatment using QM calculations at the appropriate level of theory in order to understand more deeply the Cu(I)−Cu(I) interactions and distances in these systems is a challenging task.

EXPERIMENTAL SECTION

General Procedures. All manipulations were carried out under an atmosphere of dry argon in a glovebox (MBraun) or using standard Schlenk techniques, unless stated otherwise. Diethyl ether, hexane, CH_2Cl_2, and THF were dried using an MBraun SPS-800 solvent purification system. Deuterated solvents were purchased from Deutero GmbH or Aldrich. CD_2Cl_2 was stirred over CaH_2 and then degassed three times through freeze−pump−thaw cycles prior to use. Celite was dried at 150 °C in the oven for 1 week. NMR spectra were recorded on Bruker AC200-300, Bruker ARX250, Bruker DRX300, Bruker DRX500, and Bruker DRX600 spectrometers. The chemical shifts are given in parts per million and are referenced to the deuterated solvent used for ^{1}H and ^{13}C NMR. Mass spectra were recorded on JEOL JMS-700 and Finnigan TSQ700 spectrometers and a Bruker ApexQe Apollo II FT-ICR instrument. Elemental analyses were performed in the "Mikroanalytisches Laboratorium der Chemischen Institute der Universität Heidelberg".

[Cu$_2${μ-(1a)-κ^2C,P}$_2$](PF$_6$)$_2$ (2a). To a solution of [Cu(CH$_3$CN)$_4$]-PF$_6$ (82.3 mg, 0.22 mmol) in freshly distilled and degassed CH_2Cl_2 (5 mL) was added ^{Me}NHCP^{tBu} (**1a**; 50.0 mg, 0.22 mmol) portionwise, and the reaction mixture was stirred overnight. A colorless solid was formed. The slightly yellowish supernatant was removed via filter cannula, and the precipitate was washed with THF (3 × 5 mL). **3** was obtained as a colorless solid in 80% yield (76.5 mg, 0.09 mmol). Crystals suitable for X-ray analysis were obtained by slow condensation of THF onto a concentrated solution of **3** in CH_3CN. ^{1}H NMR (300.5 MHz, CD_3CN): δ 7.48 (d, $^3J_{H,H}$ = 1.8 Hz, Im-C*H*4/5, 1H), 7.36 (d, $^3J_{H,H}$ = 1.5 Hz, Im-C*H*4/5, 1H), 3.84 (s, N(C*H*$_3$), 3H), 1.32 (d, $^1J_{H,P}$ = 15.2 Hz, P(C(C*H*$_3$)$_3$)$_2$), 18H). ^{31}P NMR (121.7 MHz, CD_3CN): δ 93.6 (s, *P*(C(CH$_3$)$_3$)$_2$), −144.6 (sep, $^1J_{P,F}$ = 706.4 Hz, *P*F$_6$). ^{13}C NMR (75.5 MHz; CD_3CN): δ 190.4 (bs, C$_{carbene}$), 126.2 (s, Im-*C*4/5), 124.7 (s, Im-C4/5), 39.1 (s, N(*C*H$_3$)), 37.7 (d, $^1J_{C,P}$ = 5.79 Hz, P(*C*(CH$_3$)$_3$)$_2$), 29.2 (s, P(C(*C*H$_3$)$_3$)$_2$). MS (FAB$^+$) *m*/*z* (%): 518.3 [M − 2PF$_6$ − Cu + 2H]$^+$; 744.5 [M − PF$_6$ + H + F]$^+$ (30). Anal. Calcd for C$_{24}$H$_{46}$Cu$_2$F$_{12}$N$_4$P$_4$: C, 33.15; H, 5.33; N, 6.44. Found: C, 32.95; H, 5.19; N, 6.69.

[Cu$_2${μ-(1b)-κ^2C,P}$_2$](PF$_6$)$_2$ (2b). In a Schlenk tube [Cu-(CH$_3$CN)$_4$]PF$_6$ (58.8 mg, 0.15 mmol) was suspended in THF (5 mL). NHCP ligand **1b** (50.0 mg, 0.15 mmol) was added in portions. After vigorous stirring for 4 h the solvent was removed under vacuum. The remaining yellow solid was dissolved in CH_2Cl_2 (2 mL), and Et_2O was added to precipitate the product as a colorless solid. The supernatant liquid was removed via filter cannula. The residue was washed with Et_2O (3 × 5 mL) and dried under vacuum, giving **2b** as a colorless solid in 85% yield (69.8 mg, 0.06 mmol). Crystals suitable for X-ray analysis were obtained by slow condensation of Et_2O onto a concentrated solution of **2b** in CH_2Cl_2. ^{1}H NMR (500.1 MHz; CD_2Cl_2): δ 7.70 (s, Im-C*H*4/5, 1H), 7.51 (s, Im-C*H*4/5, 1H), 7.09 (s, C*H*-Mes, 2H), 2.36 (s, *p*-C*H*$_3$-Mes, 3H), 2.02 (s, *o*-C*H*$_3$-Mes, 6H), 1.23 (d, $^3J_{H,P}$ = 16.5 Hz, P(C(C*H*$_3$)$_3$)$_2$), 18H). ^{31}P NMR (202.5 MHz, CD_2Cl_2): δ 107.5 (s, *P*C(CH$_3$)$_3$)$_2$), −144.6 (sep, $^1J_{P,F}$ = 710.8 Hz, *P*F$_6$). ^{13}C NMR (125.8 MHz; CD_2Cl_2): δ 185.4 (bs, C$_{carbene}$), 142.1 (s, C$_{quart}$-Mes), 135.2 (s, C$_{quart}$-Mes), 133.9 (s, C$_{quart}$-Mes), 130.4 (s, CH-Mes), 127.2 (s, Im-C4/5), 125.5 (s, Im-C4/5), 37.6 (d, $^1J_{C,P}$ = 9.1 Hz, P(*C*(CH$_3$)$_3$)$_2$), 28.8 (s, P(C(*C*H$_3$)$_3$)$_2$), 21.4 (*p*-*C*H$_3$-Mes), 18.0 (*o*-*C*H$_3$-Mes). MS (ESI$^+$) *m*/*z* (%): 931.3 (13) [M − PF$_6$]. Anal. Calcd for C$_{40}$H$_{62}$Cu$_2$F$_{12}$N$_4$P$_4$: C, 44.57; H, 5.80; N, 5,20. Found: C, 44.60; H, 5.91; N, 5.97.

[Cu(1c)$_2$](PF$_6$) (3). A solution of **1c** (50.0 mg, 0.18 mmol) in 3 mL of THF was added to a suspension of [Cu(CH$_3$CN)$_4$PF$_6$] (33.5 mg, 0.09 mmol) in 5 mL of THF. The solution was stirred overnight. A small amount of precipitate was formed, which was filtered off, and the filtrate was concentrated under vacuum to a volume of ca. 1 mL. Hexane (5 mL) was added to the solution to precipitate **3** as a colorless solid. After the supernatant was removed via filter cannula, **3** was washed with Et_2O (3 × 5 mL) and dried under vacuum, resulting in 92% yield (61.8 mg, 0.08 mmol). Crystals suitable for X-ray analysis were obtained by the condensation of hexane onto a concentrated solution of **3** in THF. ^{1}H NMR (301.5 MHz, CD_2Cl_2): δ 7.35−7.32 (m, Im-C*H*4/5, 2H), 1.75 (s, N(C(C*H*$_3$)$_3$), 9H), 1.23 (d, $^3J_{H,P}$ = 12.6 Hz, P(C(C*H*$_3$)$_3$)$_2$), 18H), ^{31}P{^{1}H} NMR: (122.7 MHz, CD_2Cl_2): δ 101.6 (s, P(C(CH$_3$)$_3$)$_2$), −144.5 (sep, $^1J_{P,F}$ = 710.2 Hz, *P*F$_6$). ^{13}C NMR (150.9 MHz; CD_2Cl_2): δ 185.5 (d, $^2J_{C,P}$ = 76.7 Hz, C$_{carbene}$), 123.1 (d, $^2J_{C,P}$ = 7.4 Hz, Im-C4), 120.6 (d, $^3J_{C,P}$ = 1.9 Hz, Im-C5), 58.3 (s, N(*C*(CH$_3$)$_3$)), 35.4 (d, $^1J_{C,P}$ = 29.2 Hz, P(*C*(CH$_3$)$_3$)$_2$), 31.8 (s, N(C(*C*H$_3$)$_3$), 29.1 (d, $^2J_{C,P}$ = 15.8 Hz, P(C(*C*H$_3$)$_3$)$_2$). MS (HR ESI$^+$), *m*/*z*: calcd for C$_{30}$H$_{58}$CuN$_4$P$_2$ 599.3433, found 599.3430. Anal. Calcd for C$_{30}$H$_{58}$CuF$_6$N$_4$P$_3$: C, 48.35; H, 7.84; N, 7.52. Found: C, 48.55; H, 8.06; N, 7.63.

[Cu$_2${μ-(1a)-κ^2C,P}$_2$]Br$_2$ (4a). To a suspension of CuBr·S(CH$_3$)$_2$ (45.2 mg, 0.22 mmol) in THF (5 mL) was added ligand **1a** (50.0 mg, 0.22 mmol) in portions; the reaction mixture was stirred overnight, and the volatiles were removed under vacuum. The residue was dissolved in CH_2Cl_2, and Et_2O (5 mL) was added to the solution to precipitate **4a**. The slightly yellowish supernatant was removed via filter cannula, and the residue was washed with Et_2O (3 × 5 mL) and dried under vacuum. **4a** was obtained as a colorless solid in 89% yield (73.2 mg, 0.10 mmol). Crystals suitable for X-ray analysis were obtained by slow condensation of hexane into a concentrated solution of **4a** in THF. ^{1}H NMR (500.1 MHz; CD_2Cl_2): δ 7.26 (d, $^3J_{H,H}$ = 1.6 Hz, Im-C*H*4/5, 1H), 7.06 (s, Im-C*H*4/5, 1H), 3.96 (s, N(C*H*$_3$), 3H), 1.44 (d, $^3J_{H,P}$ = 14.3 Hz, P(C(C*H*$_3$)$_3$)$_2$), 18H). ^{31}P NMR (202.5 MHz; CD_2Cl_2): δ 91.4 (s, *P*(C(CH$_3$)$_3$)$_2$). ^{13}C NMR (125.9 MHz; CD_2Cl_2): δ 195.2 (bs, C$_{carbene}$), 123.5 (s, Im-C4/5), 122.8 (s, Im-C4/5), 38.5 (s, P(*C*(CH$_3$)$_3$)$_2$), 37.1 (s, N(*C*H$_3$)), 29.4 (s, P(C(*C*H$_3$)$_3$)$_2$). MS (FAB$^+$), *m*/*z* (%): 515.5 [M − Cu − 2Br]$^+$ (20); 659.4 [M − Br]$^+$ (80). MS (LIFDI), *m*/*z* (%): 737.9 [M − 2H]. Anal. Calcd for C$_{24}$H$_{46}$Br$_2$Cu$_2$N$_4$P$_2$: C, 38.98; H, 6.27; N, 7.58. Found: C, 39.07; H, 6.03; N, 7.58.

[Cu$_4${μ-(1b)-κ^2C,P}$_2$](μ_4-Br)$_2$(μ_2-Br)$_2$ (4b). In a Schlenk tube CuBr·S(CH$_3$)$_2$ (61.0 mg, 0.30 mmol) was suspended in THF (5 mL). NHCP ligand **1b** (50.0 mg, 0.15 mmol) was added portionwise. After vigorous stirring for 4 h the solvent was removed under vacuum. The remaining solid was dissolved in CH_2Cl_2 (2 mL), and Et_2O was added to precipitate the product as a colorless solid. The supernatant was removed via filter cannula. The residue was washed with Et_2O (3 × 5 mL) and dried under vacuum, giving **4b** as a colorless solid in 91% yield (84.5 mg, 0.07 mmol). Crystals suitable for X-ray analysis were obtained by slow condensation of a hexane onto a concentrated solution of **4b** in THF. ^{1}H NMR (300.1 MHz, CD_2Cl_2): δ 7.33 (d, *J* = 1.9 Hz, Im-C*H*4/5, 1H), 6.92−6.90 (m, Im-C*H*4/5, C*H*-Mes, 3H), 2.27 (s, *p*-C*H*$_3$-Mes, 3H), 1.96 (s, *o*-C*H*$_3$-Mes, 3H), 1.34 (d, $^3J_{H,P}$ = 14.7 Hz, P(C(C*H*$_3$)$_3$)$_2$), 18H). ^{31}P{^{1}H} NMR (101.3 MHz, CD_2Cl_2): δ 85.5 (bs, *P*(C(CH$_3$)$_3$)$_2$)). ^{13}C NMR (75.5 MHz; CD_2Cl_2): δ 139.1 (s, C$_{quart}$-Mes), 135.8 (s, C$_{quart}$-Mes), 135.5 (s, C$_{quart}$-Mes), 129.7 (m,

dx.doi.org/10.1021/om300701u | *Organometallics* 2012, 31, 8000−8011

CH-Mes), 124.1 (m, Im-C4/5), 123.4 (m, Im-C4/5), 37.8 (d, $^1J_{C,P}$ = 1,9 Hz, P(C(CH$_3$)$_3$)$_2$), 29.4 (s, P(C(CH$_3$)$_3$)$_2$), 29.0 (s, P(C(CH$_3$)$_3$)$_2$), 21.8 (*p*-CH$_3$-Mes), 18.5 (*o*-CH$_3$-Mes); C$_{carbene}$ could not be detected. HRMS (FAB$^+$), *m*/*z*: calcd for $C_{40}H_{62}Br_3Cu_4N_4P_2$ 1154.9133, found 1154.9161. Anal. Calcd for $C_{40}H_{62}Br_4Cu_4N_4P_2$: C, 38.91; H, 5.06; N, 4.54. Found: C, 38.40; H, 4.82; N, 4.37.

[Cu$_2${*μ*-(5a)-*κ*^{2}*C*,*P*}$_2$](PF$_6$)$_2$ (6a). In a Schlenk tube [Cu(CH$_3$CN)$_4$PF$_6$] (67.0 mg, 0.18 mmol) was suspended in 5 mL of THF. A solution of **5a** (50.0 mg, 0.18 mmol) in THF (2 mL) was added dropwise, and the reaction mixture was stirred for 3 h. The solvent was removed under vacuum. The residue was redissolved in CH_2Cl_2 (2 mL). After the addition of Et_2O (5 mL) a colorless solid was formed. The yellowish supernatant was removed via filter cannula. The remaining product was washed with Et_2O (3 × 5 mL) and dried under vacuum, resulting in 66% yield (58.3 mg). Crystals suitable for X-ray analysis were obtained by slow evaporation of a concentrated CH_2Cl_2 solution. ^{1}H NMR (300.1 MHz, CD_2Cl_2): *δ* 7.42 (bs, Im-C*H*4/5, 1H), 7.27 (bs, Im-C*H*4/5, 1H), 4.98 (d, $^2J_{P,H}$ = 18.4 Hz, P(C*H*$_2$), 1H), 4.49 (d, $^2J_{P,H}$ = 15.8 Hz, P(C*H*$_2$), 1H), 1.65 (s, N(C(C*H*$_3$)$_2$), 18H), 1.35 ("t", $^3J_{P,H}$ = 7.21 Hz, P(C(C*H*$_3$)$_3$)$_2$), 9H), 1.20 ("t", $^3J_{P,H}$ = 7.2 Hz, P(C(C*H*$_3$)$_3$)$_2$), 9H). ^{31}P NMR (101.3 MHz, CD_2Cl_2): *δ* 48.0 (s, *P*((C(CH$_3$)$_3$)$_2$), −144.6 (sep, $^1J_{P,F}$ = 707.9 Hz, *P*F$_6$). ^{13}C NMR (75.5 MHz, CD_2Cl_2): *δ* 170.0 (s, C$_{carbene}$), 124.2 (s, Im-C4/5), 119.7 (s, Im-C4/5), 58.3 (s, N(C(CH$_3$)$_3$)), 43.8 ("t", $^1J_{C,P}$ = 11.9 Hz, P(*C*H$_2$)), 34.3 (d, $^1J_{C,P}$ = 6.13 Hz, P(*C*(CH$_3$)$_3$)$_2$), 33.9 ("t", $^1J_{C,P}$ = 8.1 Hz, P(*C*(CH$_3$)$_3$)$_2$), 31.4 (s, N(C(*C*H$_3$)$_3$)), 29.1 ("t", $^2J_{C,P}$ = 2.82 Hz, P(C(*C*H$_3$)$_3$)$_2$), 28.6 ("t", $^2J_{C,P}$ = 3.0 Hz, P(C(CH$_3$)$_3$)$_2$). Anal. Calcd for $C_{32}H_{62}F_{12}N_4P_4Cu_2$: C, 39.15; H, 6.37; N, 5.71. Found: C, 39.19; H, 6.50; N, 5.77.

[Cu$_2${*μ*-(5b)-*κ*^{2}*C*,*P*}$_2$](PF$_6$)$_2$ (6b). To a suspension of [Cu(CH$_3$CN)$_4$PF$_6$] (54.0 mg, 0.15 mmol) in THF (5 mL) was added a solution of **5b** (50.0 mg, 0.15 mmol) in THF (2 mL) dropwise. A clear yellowish solution was formed. After 4 h of vigorous stirring Et_2O (5 mL) was added to precipitate the product. The yellow supernatant was removed via filter cannula. The precipitate was redissolved in CH_2Cl_2, and another 5 mL of Et_2O was added. The supernatant was removed, and the product was washed with Et_2O (3 × 5 mL) and dried under vacuum, resulting in a 65% yield (52.3 mg, 0.05 mmol). Crystals suitable for X-ray analysis were obtained by slow evaporation of a concentrated solution in CH_2Cl_2. ^{1}H NMR (500.1 MHz; CD_2Cl_2; 295 K): *δ* 7.55 (s, Im-C*H*4/5, 1H), 7.04 (s, Im-C*H*4/5, 1H), 7.00 (s, C*H*-Mes, 2H), 4.91 (s, P(C*H*$_2$), 2H), 2.32 (s, *p*-C*H*$_3$-Mes-CH$_3$, 3H), 1.96 (s, *o*-C*H*$_3$-Mes, 6H), 1.10 (d, $^3J_{C,P}$ = 14.4 Hz, P(C(C*H*$_3$)$_2$), 18H). ^{1}H NMR (500.1 MHz; CD_2Cl_2; 183 K): *δ* 7.17 (bs, Im-C*H*4/5, 1H), 6.84 (bs, Im-C*H*4/5, 1H), 6.77 (s, C*H*-Mes, 2H), 4.09 (bs, P(C*H*$_2$), 1H), 3.46 (bs, P(C*H*$_2$), 1H), 2.18 (bs, *p*-C*H*$_3$-Mes, 3H), 1.57 (bs, *o*-C*H*$_3$-Mes, 3H), 1.31 (bs, *o*-CH$_3$-Mes, 3H), 0.99 (bs, P(C(C*H*$_3$)$_3$)$_2$), 9H), 0.61 (bs, *P*(C(C*H*$_3$)$_3$)$_2$), 9H). ^{31}P{^{1}H} NMR (202.5 MHz, CD_2Cl_2): *δ* 47.7 (s, *P*(CH$_2$)), −144.6 (sep, $^1J_{P,F}$ = 711.5 Hz, *P*F$_6$). ^{13}C NMR (151.8 MHz; CD_2Cl_2): *δ* 141.5 (s, C$_{quart}$-Mes), 135.3 (s, C$_{quart}$-Mes), 135.2 (s, C$_{quart}$-Mes), 130.3 (s, *C*H-Mes), 125.9 (s, Im-C4/5), 123.7 (s, Im-C4/5), 43.7 (d, $^1J_{C,P}$ = 20.9 Hz, P(*C*H$_2$)), 35.0 (d, $^1J_{C,P}$ = 15.2 Hz, P(*C*(CH$_3$)$_3$)$_2$), 29.7 (d, $^2J_{C,P}$ = 5.1 Hz, P(C(*C*H$_3$)$_3$)$_2$), 21.3 (s, *p*-*C*H$_3$-Mes), 18.2 (s, *o*-*C*H$_3$-Mes). ^{1}H-VT NMR (500.1 MHz, CD_2Cl_2): P(CH$_2$), T_c = 243 ± 5 K, k_c = 659 Hz. MS (ESI$^+$), *m*/*z* (%): 345.3 (100) [(**5b**) + H], 985.2 (25) [M − Mesityl]. Anal. Calcd for $C_{42}H_{66}Cu_2F_{12}N_4P_4$: C, 45.61, H, 6.02; N, 5.07. Found: C, 45.61; H, 6.00; N, 4.79.

[Cu$_2${*μ*-(BIM^{tBu}-*κ*^{2}*C*,*P*}$_2$] (10a). *Method A.* To a stirred suspension of imidazolium salt **9** (0.30 g, 0.54 mmol) in THF (6 mL) at −78 °C was added a 1.78 M solution of *n*BuLi in hexane (0.62 mL, 1.10 mmol). The reaction mixture was warmed to room temperature, and a clear solution was obtained. After the mixture was stirred at ambient temperature for 15 min, a colorless solid precipitated. The suspension was further stirred for 10 min and added via a syringe (equipped with an appropriately thick needle) to a suspension of [Cu(MeCN)$_4$]PF$_6$ cooled to −78 °C (0.21 g, 0.57 mmol) in THF (6 mL). The suspension was stirred at room temperature for 2 h, and the solvent was removed under vacuum. The residue was treated with CH_2Cl_2 (12 mL) and vigorously stirred, and the solid was allowed to precipitate overnight. The clear solution was transferred via filter cannula into a separate Schlenk tube and concentrated under vacuum to a volume of ca. 6−7 mL. The solution was carefully layered with Et_2O (20 mL) and allowed to stand at ambient temperature for several days. The precipitated compound was separated from the solvents and dried under vacuum to give 170 mg of **10a** as a white powder, mp 243−244 °C dec. The product obtained was slightly (5−6 mol %) contaminated with LiPF$_6$, as was established by elemental analysis. In the solid state, compound **10a** is moderately sensitive to air. Crystals of **10a** suitable for X-ray analysis were obtained by slow evaporation of a CH_2Cl_2 solution of the product. ^{1}H NMR (500.1 MHz, CD_2Cl_2, 295 K): *δ* 7.51 (bs, Im-C*H*4/5, 4H), 7.35 (d, $^3J_{H,H}$ = 2.1 Hz, Im-C*H*4/5, 4H), 6.48 (bs, C*H*$_2$, 4H), 1.65 (s, N(C(C*H*$_3$)$_3$), 36H). ^{31}P NMR (202.5 MHz, acetone-*d*$_6$, 295 K): *δ* −143.5 (sep, $^1J_{P,F}$ = 708 Hz, PF$_6$). ^{13}C NMR (125.8 MHz, CD_2Cl_2, 295 K): 174.2 (s, C$_{carbene}$), 122.1, 120.7 (all bs, Im-C4/5), 65.9 (s, N(*C*H$_2$)), 59.0 (s, N(*C*(CH$_3$)$_3$)), 31.8 (s, N(C(*C*H$_3$)$_3$)). Spectroscopic data for **10a** at low temperature are as follows. ^{1}H NMR (500.1 MHz, CD_2Cl_2, 213 K): *δ* 7.57 (s, Im-C*H*4/5, 2H), 7.46 (s, Im-C*H*4/5, 2H), 7.33 (s, Im-C*H*4/5, 2H), 7.24 (s, Im-C*H*4/5, 2H), 6.51 (d, $^2J_{H,H}$ = 13.9 Hz, CH$_2$, 2H), 6.20 (d, $^2J_{H,H}$ = 13.9 Hz, N(C*H*$_2$), 2H), 1.66 (s, N(C(C*H*$_3$)$_3$), 18H), 1.47 (s, N(C(C*H*$_3$)$_3$), 18H). ^{13}C NMR (125.8 MHz, CD_2Cl_2, 234 K): *δ* 173.9, 172.4 (all s, C$_{carbene}$), 122.2, 121.4, 121.3, 118.8 (all s, Im-C4/5), 64.9 (s, N(CH$_2$)), 58.4, 58.2 (all s, N(*C*(CH$_3$)$_3$)), 31.7, 30.6 (all s, N(C(*C*H$_3$)$_3$)). ^{1}H-VT NMR (500.1 MHz, CD_2Cl_2): Im-H, T_c = 256 ± 4 K, k_c = 100 Hz; Im-H, T_c = 265 ± 4 K, k_c = 127.4 Hz; *t*Bu, T_c = 265 ± 4 K, k_c = 215 Hz; CH$_2$, T_c = 277 ± 4 K, k_c = 352 Hz. MS-FAB (NBA): *m*/*z* 791.5 (70%) [(M − PF$_6$)$^+$], 323 (100%) {[(1/2M) − PF$_6$]$^+$}, correct isotopic pattern.

Method B. Imidazolium salt **9** (0.40 g, 0.72 mmol) and KO*t*Bu (0.17 g, 1.56 mmol) were suspended in absolute THF (6 mL) at −20 °C. The brown suspension was warmed to room temperature, stirred at ambient temperature for 30 min, and then added via syringe to a to −40 °C cooled suspension of [Cu(CH$_3$CN)$_4$]PF$_6$ (0.32 mg, 0.87 mmol) in THF (7 mL). The reaction mixture was stirred for 1 h at 25 °C and then evaporated under vacuum. CH_2Cl_2 (15 mL) was added, the reaction mixture was vigorously stirred for 10 min, and then the solid was allowed to precipitate. The supernatant was carefully transferred via a filter cannula into a separate Schlenk tube and evaporated to give a crude, brownish product. Although precipitation by Et_2O as described above did enhance the purity of **10a**, method A seems to be more suitable for the synthesis of complex **10a**.

[Cu$_2${*μ*-(BIM^{tBu}-B(CH$_3$)$_2$-*κ*^{2}*C*,*P*}$_2$] (10b). To a suspension of salt **8b** (1.00 g, 2.73 mmol) and CuBr (0.39 g, 2.73 mmol) in THF (10 mL) at −70 °C was added a hexane solution of *n*BuLi (3.10 mL, 5.49 mmol). The reaction mixture was stirred at room temperature overnight, and all volatiles were removed under vacuum. The residue was treated with CH_2Cl_2 (15 mL), vigorously stirred, centrifuged under Ar (1800 rpm; 60 min), and allowed to stand for 3 days at ambient temperature. The clear, slightly brownish supernatant was transferred via filter cannula into a separate Schlenk tube. The solution was concentrated to ca. one-third of the initial volume, carefully layered with pentane (30 mL), and allowed to stand at ambient temperature for 1 week. The precipitated product was separated and dried under vacuum. Yield: 175 mg. Purity: ca. 85−90%. ^{1}H NMR (500.1 MHz, CD_2Cl_2, 298 K): *δ* 7.01 (s, Im-C*H*4/5, 4H), 7.00 (s, Im-C*H*4/5, 4H), 1.59 (s, 36H, N(C(CH$_3$)$_3$)), 0.46 (s, 12H, B(CH$_3$)$_2$). ^{13}C NMR (125.8 MHz, CD_2Cl_2, 298 K): *δ* 178.3 (s, C$_{carbene}$), 122.5, 115.7 (all s, Im-C), 56.0 (s, N(C(CH$_3$)$_3$)), 32.2 (s, N(C(CH$_3$)$_3$)), 14.9 (bs, B(CH$_3$)$_2$). Spectroscopic data for compound **10b** at low temperature are as follows. ^{1}H NMR (500.1 MHz, CD_2Cl_2, 194 K): *δ* 7.09 (s, Im-C*H*4/5, 2H), 7.04 (s, Im-C*H*4/5, 2H), 7.00 (s, Im-C*H*4/5, 2H), 6.87 (s, Im-C*H*4/5, 2H), 1.65 (s, N(C(C*H*$_3$)$_3$), 18H), 1.36 (s, N(C(C*H*$_3$)$_3$), 18H), 0.62 (s, B(C*H*$_3$)$_2$, 3H) 0.12 (s, B(C*H*$_3$)$_2$, 3H). ^{13}C NMR (125.8 MHz, CD_2Cl_2, 213 K): *δ* 176.8, 176.5 (all s, C$_{carbene}$), 122.0, 121.1, 116.1, 114.7 (all s, Im-C4/5), 55.7, 55.2 (all s, N(C(CH$_3$)$_3$)), 31.7, 31.0 (all s, N(C(CH$_3$)$_3$)), 15.1 (bs, B(CH$_3$)$_2$), 12.6 (bs, B(CH$_3$)$_2$). ^{1}H-VT NMR (500.1 MHz, CD_2Cl_2): *t*Bu, T_c = 245 ± 4 K, k_c = 329 Hz; B(CH$_3$)$_2$, T_c = 251 ± 4 K, k_c = 549.5 Hz; temperature calibration by external MeOH. MS-FAB (NBA): *m*/*z*

dx.doi.org/10.1021/om300701u | *Organometallics* 2012, 31, 8000−8011

351.4 (80%) [($^1/_2$M + H)$^+$], 661.5 (5%) [(MH_2 − BMe_2)$^+$], 700.6 (3%) [M$^+$].

X-ray Diffraction Studies. For the X-ray diffraction studies, data sets were collected on Bruker "Smart CCD" diffractometers for **2a**, **6a,b**, and **10b**, "APEX" instruments for **2b**, **3**, **4b**, and **10a**, and "APEX-II" instruments for **4a** with Mo Kα radiation (λ = 0.710 73 Å). A complete sphere in reciprocal space was covered by 0.3° ω scans in all cases. For all data sets, the intensities were corrected for Lorentz and polarization effects, and an empirical absorption correction, based on the Laue symmetry of the reciprocal space, was applied using SADABS (2008/1).[27] All structures were solved by direct methods and refined against F^2 with a full-matrix least-squares algorithm using the SHELXTL (version 2008/4)[28] software package. All hydrogen atoms were treated using appropriate riding models.

Crystal data for **2a**: colorless crystal (polyhedron), dimensions 0.40 × 0.26 × 0.16 mm^3, crystal system monoclinic, space group $P2_1/n$, Z = 2, a = 7.8986(1) Å, b = 11.0020(2) Å, c = 20.4886(1) Å, α = 90°, β = 97.825(1)°, γ = 90°, V = 1763.89(4) Å^3, ρ = 1.637 g/cm^3, T = 200(2) K, θ_{max} = 27.48°, 17 443 reflections measured, 4043 unique (R_{int} = 0.0527), 3666 observed ($I > 2\sigma(I)$), 279 parameters refined, hydrogen atoms treated using appropriate riding models, goodness of fit 1.07 for observed reflections, final residual values R1(F) = 0.034, wR2(F^2) = 0.089 for observed reflections, residual electron density −0.50 to 1.29 e Å^{-3}.

Crystal data for **2b**: colorless crystal (needle), dimensions 0.46 × 0.07 × 0.07 mm^3, crystal system triclinic, space group $P\bar{1}$, Z = 2, a = 10.5350(4) Å, b = 14.1754(5) Å, c = 18.8638(7) Å, α = 82.406(1)°, β = 81.660(1)°, γ = 72.915(1)°, V = 2652.32(17) Å^3, ρ = 1.456 g/cm^3, T = 200(2) K, θ_{max} = 25.05°, 22 758 reflections measured, 9253 unique (R_{int} = 0.0512), 6857 observed ($I > 2\sigma(I)$), 678 parameters refined, hydrogen atoms treated using appropriate riding models, goodness of fit 1.02 for observed reflections, final residual values R1(F) = 0.050, wR2(F^2) = 0.117 for observed reflections, residual electron density −0.52 to 0.44 e Å^{-3}.

Crystal data for **3**: colorless crystal (polyhedron), dimensions 0.19 × 0.19 × 0.15 mm^3, crystal system monoclinic, space group $P2_1/c$, Z = 4, a = 10.3816(7) Å, b = 15.9198(11) Å, c = 23.8645(17) Å, α = 90°, β = 91.222(2)°, γ = 90°, V = 3943.3(5) Å^3, ρ = 1.255 g/cm^3, T = 200(2) K, θ_{max} = 27.04°, 37 253 reflections measured, 8335 unique (R_{int} = 0.0754), 6005 observed ($I > 2\sigma(I)$), μ = 0.73 mm^{-1}, T_{min} = 0.87, T_{max} = 0.90, goodness of fit 1.10 for observed reflections, final residual values R1(F) = 0.074, wR2(F^2) = 0.175 for observed reflections, residual electron density −0.57 to 0.76 e Å^{-3}.

Crystal data for **4a**: colorless crystal (polyhedron), dimensions 0.14 × 0.11 × 0.11 mm^3, crystal system monoclinic, space group $P2_1/n$, Z = 4, a = 11.7472(7) Å, b = 19.7890(11) Å, c = 14.3583(8) Å, α = 90°, β = 109.438(1)°, γ = 90°, V = 3147.6(3) Å^3, ρ = 1.561 g/cm^3, T = 200(2) K, θ_{max} = 30.46°, 41 785 reflections measured, 9529 unique (R_{int} = 0.0357), 7337 observed ($I > 2\sigma(I)$), goodness of fit 1.02 for observed reflections, final residual values R1(F) = 0.030, wR2(F^2) = 0.065 for observed reflections, residual electron density −1.11 to 0.89 e Å^{-3}.

Crystal data for **4b**: dolorless crystal (polyhedron), dimensions 0.22 × 0.19 × 0.18 mm^3, crystal system monoclinic, space group $P2_1/c$, Z = 2, a = 12.1724(11) Å, b = 15.2240(14) Å, c = 14.9025(14) Å, α = 90°, β = 94.477(2)°, γ = 90°, V = 2753.2(4) Å^3, ρ = 1.632 g/cm^3, T = 200(2) K, θ_{max} = 28.37°, 28 870 reflections measured, 6861 unique (R_{int} = 0.0397), 5445 observed ($I > 2\sigma(I)$), μ = 4.59 mm^{-1}, T_{min} = 0.43, T_{max} = 0.49, goodness of fit 1.04 for observed reflections, final residual values R1(F) = 0.032, wR2(F^2) = 0.083 for observed reflections, residual electron density −0.48 to 0.91 e Å^{-3}.

Crystal data for **6a**: colorless crystal (plate), dimensions 0.28 × 0.10 × 0.02 mm^3, crystal system monoclinic, space group $C2/c$, Z = 8, a = 24.7326(1) Å, b = 11.3777(2) Å, c = 20.7465(4) Å, α = 90°, β = 112.9140(10)°, γ = 90°, V = 5377.39(14) Å^3, ρ = 1.423 g/cm^3, T = 200(2) K, θ_{max} = 20.69°, 13 904 reflections measured, 2767 unique (R_{int} = 0.0831), 2068 observed ($I > 2\sigma(I)$), goodness of fit 1.10 for observed reflections, final residual values R1(F) = 0.100, wR2(F^2) = 0.273 for observed reflections, residual electron density −1.01 to 1.95 e Å^{-3}.

Crystal data for **6b**: colorless crystal (plate), dimensions 0.30 × 0.16 × 0.06 mm^3, crystal system monoclinic, space group $C2/c$, Z = 8, a = 24.8999(7) Å, b = 25.0763(7) Å, c = 21.3452(6) Å, α = 90°, β = 122.457(1)°, γ = 90°, V = 11 246.0(5) Å^3, ρ = 1.457 g/cm^3, T = 200(2) K, θ_{max} = 23.82°, 8635 unique (R_{int} = 0.0857), 6129 observed ($I > 2\sigma(I)$), 724 parameters refined, goodness of fit 1.04 for observed reflections, final residual values R1(F) = 0.051, wR2(F^2) = 0.121 for observed reflections, residual electron density −0.61 to 0.87 eÅ^{-3}.

Crystal data for **10a**: colorless crystal (polyhedron), dimensions 0.22 × 0.18 × 0.13 mm^3, crystal system triclinic, space group $P\bar{1}$, Z = 2, a = 11.6179(7) Å, b = 12.9619(8) Å, c = 16.0697(10) Å, α = 80.063(1)°, β = 84.338(1)°, γ = 73.271(1)°, V = 2279.7(2) Å^3, ρ = 1.614 g/cm^3, T = 100(2) K, θ_{max} = 28.33°, 24 060 reflections measured, 11 225 unique (R_{int} = 0.0258), 8803 observed ($I > 2\sigma(I)$), 541 parameters refined, hydrogen atoms treated using appropriate riding models, goodness of fit 1.01 for observed reflections, final residual values R1(F) = 0.036, wR2(F^2) = 0.078 for observed reflections, residual electron density −0.37 to 0.60 e Å^{-3}.

Crystal data for **10b**: colorless crystal (polyhedron), dimensions 0.22 × 0.11 × 0.09 mm^3, crystal system triclinic, space group $P\bar{1}$, Z = 2, a = 9.7721(10) Å, b = 11.8877(12) Å, c = 16.7399(17) Å, α = 85.132(2)°, β = 88.307(2)°, γ = 66.628(2)°, V = 1778.6(3) Å^3, ρ = 1.310 g/cm^3, T = 100(2) K, θ_{max} = 27.16°, 17 327 reflections measured, 7824 unique (R_{int} = 0.0405), 5647 observed ($I > 2\sigma(I)$), μ = 1.23 mm^{-1}, T_{min} = 0.77, T_{max} = 0.90, 413 parameters refined, goodness of fit 0.99 for observed reflections, final residual values R1(F) = 0.041, wR2(F^2) = 0.088 for observed reflections, residual electron density −0.36 to 0.69 e Å^{-3}.

■ ASSOCIATED CONTENT

Ⓢ Supporting Information

Text giving details of the synthesis of BIM-BMe_2, figures giving NMR spectra, and CIF files giving crystallographic data for all crystal structure determinations. This material is available free of charge via the Internet at http://pubs.acs.org.

■ AUTHOR INFORMATION

Corresponding Author

*E-mail: ph@oci.uni-heidelberg.de.

Notes

The authors declare no competing financial interest.

■ ACKNOWLEDGMENTS

Support of this work by the Deutsche Forschungsgemeinschaft (through SFB 623 "Molecular Catalysts: Structure and Functional Design") and by a fellowship of the Graduate College 850 ("Modeling of Molecular Properties") to E.K. is gratefully acknowledged.

■ REFERENCES

(1) (a) Pyykkö, P. *Chem. Rev.* **1997**, 597. (b) Pyykkö, P.; Mendizabal, F. *Chem. Eur. J.* **1997**, *3*, 1458. (c) Pyykkö, P.; Runeberg, N.; Mendizabal, F. *Chem. Eur. J.* **1997**, *3*, 1451.

(2) (a) Pyykkö, P.; Zhao, Y. *Angew. Chem., Int. Ed.* **1991**, *30*, 604. (b) Pyykko, P. *Chem. Rev.* **1988**, *88*, 563.

(3) (a) Merz, K. M.; Hoffmann, R. *Inorg. Chem.* **1988**, *27*, 2120. (b) Mehrotra, P. K.; Hoffmann, R. *Inorg. Chem.* **1978**, *17*, 2187.

(4) (a) Fernández, E. J.; López-de-Luzuriaga, J. M.; Monge, M.; Rodríguez, M. A. *Inorg. Chem.* **1998**, *37*, 6002. (b) Poblet, J.-M.; Bénard, M. *Chem. Commun.* **1998**, 1179. (c) Carvajal, M. A.; Alvarez, S.; Novoa, J. J. *Chemistry* **2004**, *10*, 2117. (d) O'Grady, E.; Kaltsoyannis, N. *Phys. Chem. Chem. Phys.* **2004**, *6*, 680.

(5) (a) Cotton, F. A.; Feng, X.; Timmons, D. J. *Inorg. Chem.* **1998**, *37*, 4066. (b) Lee, S. W.; Trogler, W. C. *Inorg. Chem.* **1990**, *29*, 1659. (c) Cotton, F. A.; Feng, X.; Matusz, M.; Poli, R. *J. Am. Chem. Soc.* **1988**, *110*, 7077.

(6) (a) Fränkel, R.; Kniczek, J.; Ponikwar, W.; Nöth, H.; Polborn, K.; Fehlhammer, W. P. *Inorg. Chim. Acta* **2001**, *312*, 23. (b) Hu, X.; Castro-Rodriguez, I.; Meyer, K. *J. Am. Chem. Soc.* **2003**, *125*, 12237. (c) Matsumoto, K.; Matsumoto, N.; Ishii, A.; Tsukuda, T.; Hasegawa, M.; Tsubomura, T. *Dalton Trans.* **2009**, 6795. (d) Poyatos, M.; Mata, J. A.; Peris, E. *Chem. Rev.* **2009**, *109*, 3677. (e) Venkatachalam, G.; Heckenroth, M.; Neels, A.; Albrecht, M. *Helv. Chim. Acta* **2009**, 1034. (f) Ellul, C. E.; Reed, G.; Mahon, M. F.; Pascu, S. I.; Whittlesey, M. K. *Organometallics* **2010**, *29*, 4097. (g) Catalano, V. J.; Munro, L. B.; Strasser, C. E.; Samin, A. F. *Inorg. Chem.* **2011**, *50*, 8465. (h) Tubaro, C.; Biffis, A.; Gava, R.; Scattolin, E.; Volpe, A.; Basato, M.; Díaz-Requejo, M. M.; Perez, P. J. *Eur. J. Org. Chem.* **2012**, *2012*, 1367.

(7) (a) Che, C.-M.; Mao, Z.; Miskowski, V. M.; Tse, M.-C.; Chan, C.-K.; Cheung, K. K.; Phillips, D. L.; Leung, K.-H. *Angew. Chem., Int. Ed.* **2000**, *39*, 4084. (b) Mao, M. Z.; Chao, H. Y.; Che, C. M.; Fu, W. F.; Cheung, K. K.; Zhu, N. *Chem. Eur. J.* **2003**, *9*, 2885. (c) Phillips, D. L.; Che, C.-M.; Leung, K. H.; Mao, Z.; Tse, M.-C. *Coord. Chem. Rev.* **2005**, *249*, 1476.

(8) Straub, B. F.; Rominger, F.; Hofmann, P. *Inorg. Chem.* **2000**, *39*, 2113.

(9) Kühl, O. *Chem. Soc. Rev.* **2007**, *36*, 592.

(10) Albert, K.; Gisdakis, P.; Rösch, N. *Organometallics* **1998**, *17*, 1608.

(11) Herrmann, W. A.; Kocher, C.; Gooßen, L. J.; Artus, G. R. J. *Chem. Eur. J.* **1996**, *2*, 1627.

(12) Yang, C.; Lee, H. M.; Nolan, S. P. *Org. Lett.* **2001**, *3*, 1511.

(13) (a) Danopoulos, A. A.; Winston, S.; Gelbrich, T.; Hursthouse, M. B.; Tooze, R. P. *Chem. Commun.* **2002**, 482. (b) Tsoureas, N.; Danopoulos, A. A.; Tulloch, A. A. D.; Light, M. E. *Organometallics* **2003**, *22*, 4750. (c) Lee, H. M.; Chiu, P. L.; Zeng, J. Y. *Inorg. Chim. Acta* **2004**, *357*, 4313. (d) Lee, H. M.; Zeng, J. Y.; Hu, C.-H.; Lee, M.-T. *Inorg. Chem.* **2004**, *43*, 6822. (e) Wang, A.-E.; Zhong, J.; Xie, J.-H.; Li, K.; Zhou, Q.-L. *Adv. Synth. Catal.* **2004**, *346*, 595. (f) Field, L. D.; Messerle, B. A.; Vuong, K. Q.; Turner, P. *Organometallics* **2005**, *24*, 4241. (g) Wang, A.-E.; Xie, J.-H.; Wang, L.-X.; Zhou, Q.-L. *Tetrahedron* **2005**, *61*, 259. (h) Hahn, F. E.; Jahnke, M. C.; Pape, T. *Organometallics* **2006**, *25*, 5927. (i) Wolf, J.; Labande, A.; Daran, J.-C.; Poli, R. *J. Organomet. Chem.* **2006**, *691*, 433. (j) Zhou, Q.-L.; Zhong, J.; Xie, J.-H.; Wang, A.-E.; Zhang, W. *Synlett* **2006**, *8*, 1193. (k) Lee, C. C.; Ke, W. C.; Chan, K. T.; Lai, C. L.; Hu, C. H.; Lee, H. M. *Chem. Eur. J.* **2007**, *13*, 582. (l) Miranda-Soto, V.; Grotjahn, D. B.; DiPasquale, A. G.; Rheingold, A. L. *J. Am. Chem. Soc.* **2008**, *130*, 13200. (m) Shaghafi, M. B.; Kohn, B. L.; Jarvo, E. R. *Org. Lett.* **2008**, *10*, 4743. (n) Wolf, J.; Labande, A.; Daran, J.-C.; Poli, R. *Eur. J. Inorg. Chem.* **2008**, 3024. (o) Benhamou, L.; Wolf, J.; César, V.; Labande, A.; Poli, R.; Lugan, N.; Lavigne, G. *Organometallics* **2009**, *28*, 6981. (p) Hahn, F. E.; Naziruddin, R. A.; Hepp, A.; Pape, T. *Organometallics* **2010**, *29*, 5283. (q) Cabeza, J. A.; Damonte, M.; García-Álvarez, P.; Kennedy, A. R.; Pérez-Carreño, E. *Organometallics* **2011**, *30*, 826. (r) Cabeza, J. A.; Damonte, M.; García-Álvarez, P.; Hernández-Cruz, M. G.; Kennedy, A. R. *Organometallics* **2012**, *31*, 327.

(14) For chiral NHCPs see: (a) Lang, H.; Vittal, J. J.; Leung, P.-H. *Dalton Trans.* **1998**, 2109. (b) Focken, T.; Raabe, G.; Bolm, C. *Tetrahedron: Asymmetry* **2004**, *15*, 1693. (c) Helmchen, G.; Bappert, E. *Synlett* **2004**, 1789. (d) Gischig, S.; Togni, A. *Organometallics* **2004**, *23*, 2479. (e) Becht, J.-M.; Bappert, E.; Helmchen, G. *Adv. Synth. Catal.* **2005**, *347*, 1495. (f) Bolm, C.; Focken, T.; Rudolph, J. *Synthesis* **2005**, *2005*, 429. (g) Gischig, S.; Togni, A. *Eur. J. Inorg. Chem.* **2005**, *2005*, 4745. (h) Hodgson, R.; Douthwaite, R. E. *J. Organomet. Chem.* **2005**, *690*, 5822. (i) Gischig, S.; Togni, A. *Organometallics* **2005**, *24*, 203. (j) Shi, J.-C.; Yang, P.-Y.; Tong, Q.; Wu, Y.; Peng, Y. *J. Mol. Catal. A: Chem.* **2006**, *259*, 7. (k) Nanchen, S.; Pfaltz, A. *Helv. Chim. Acta* **2006**, *89*, 1559. (l) Labande, A.; Daran, J.-C.; Manoury, E.; Poli, R. *Eur. J. Inorg. Chem.* **2007**, *2007*, 1205. (m) Visentin, F.; Togni, A. *Organometallics* **2007**, *26*, 3746. (n) Shi, J. C.; Yang, P.; Tong, Q.; Jia, L. *Dalton Trans.* **2008**, 938. (o) Willms, H.; Frank, W.; Ganter, C. *Chem. Eur. J.* **2008**, *14*, 2719. (p) We have developed a new, efficient and highly modular synthetic route to enantiopure P-chiral NHCP ligands: Brill, M; Hanno-Igels, P.; Hofmann, P. Manuscript in preparation.

(15) Nägele, P.; Herrlich (née Blumbach), U.; Rominger, F.; Hofmann, P. Manuscript in preparation, 2012.

(16) Salem, H.; Herrlich (née Blumbach), U.; Kühnel, E.; Brill, M; Nägele, P.; Bogado, A. L.; Rominger, F.; Hofmann, P. *Organometallics* **2012**, submitted for publication.

(17) (a) Marchenko, A. P.; Koidan, H. N.; Huryeva, A. N.; Zarudnitskii, E. V.; Yurchenko, A. A.; Kostyuk, A. N. *J. Org. Chem.* **2010**, *75*, 7141. (b) Marchenko, A. P.; Koidan, H. N.; Pervak, I. I.; Huryeva, A. N.; Zarudnitskii, E. V.; Tolmachev, A. A.; Kostyuk, A. N. *Tetrahedron Lett.* **2012**, *53*, 494.

(18) (a) Hillier, A. C.; Sommer, W. J.; Yong, B. S.; Petersen, J. L.; Cavallo, L.; Nolan, S. P. *Organometallics* **2003**, *22*, 4322. (b) Díez-González, S.; Nolan, S. P. *Coord. Chem. Rev.* **2007**, *251*, 874. (c) Poater, A.; Cosenza, B.; Correa, A.; Giudice, S.; Ragone, F.; Scarano, V.; Cavallo, L. *Eur. J. Inorg. Chem.* **2009**, *2009*, 1759. (d) Clavier, H.; Nolan, S. P. *Chem. Commun.* **2010**, *46*, 841. (e) Droge, T.; Glorius, F. *Angew. Chem., Int. Ed.* **2010**, *49*, 6940.

(19) Tolman, C. A. *Chem. Rev.* **1977**, *77*, 313.

(20) Shishkov, I. V.; Rominger, F.; Hofmann, P. *Dalton Trans.* **2009**, 1428.

(21) Tulloch, A. A. D.; Danopoulos, A. A.; Kleinhenz, S.; Light, M. E.; Hursthouse, M. B.; Eastham, G. *Organometallics* **2001**, *20*, 2027.

(22) Schneider, N.; César, V.; Bellemin-Laponnaz, S.; Gade, L. H. *J. Organomet. Chem.* **2005**, *690*, 5556.

(23) (a) Fu, W. F.; Gan, X.; Che, C. M.; Cao, Q. Y.; Zhou, Z. Y.; Zhu, N. N. *Chem. Eur. J.* **2004**, *10*, 2228. (b) Scherer, M.; Stein, D.; Breher, F.; Geier, J.; Schönberg, H.; Grützmacher, H. *Z. Anorg. Allg. Chem.* **2005**, *631*, 2770. (c) Mézailles, N.; Le Floch, P.; Waschbüsch, K.; Ricard, L.; Mathey, F.; Kubiak, C. P. *J. Organomet. Chem.* **1997**, *541*, 277.

(24) (a) Matsumoto, K.; Matsumoto, N.; Ishii, A.; Tsukuda, T.; Hasegawa, M.; Tsubomura, T. *Dalton Trans.* **2009**, 6795. (b) Hu, X.; Castro-Rodriguez, I.; Meyer, K. *J. Am. Chem. Soc.* **2003**, 12237.

(25) Fränkel, R.; Kniczek, J.; Ponikwar, W.; Nöth, H.; Polborn, K.; Fehlhammer, W. P. *Inorg. Chim. Acta* **2001**, *312*, 23.

(26) Kühnel, E. Ongoing Ph.D. thesis, University of Heidelberg, Heidelberg, Germany.

(27) Sheldrick, G. M. *SADABS*; Bruker Analytical X-ray Division, Madison, WI, 2008.

(28) Sheldrick, G. M. *Acta Crystallogr.* **2008**, *A64*, 112.